Centre for Geo-Information

Thesis Report GIRS-2016-36

TREE CROWN SHAPE PARAMETER EXTRACTION FROM AIRBORNE PHOTOGRAMMETRIC POINT CLOUD

Christina Kallimani

December 2016

WAGENINGEN UNIVERSITY
WAGENINGEN UR

TREE CROWN SHAPE PARAMETER EXTRACTION FROM AIRBORNE PHOTOGRAMMETRIC POINT CLOUD

Christina Kallimani

860209416040

Supervisors:

Dr. Harm Bartholomeus

Dr. Juha Suomalainen

A thesis submitted in partial fulfilment of the degree of Master of Science

at Wageningen University and Research Centre,

The Netherlands

15.12.2016

Wageningen, The Netherlands

Thesis code number: GRS-80436
Thesis Report: GIRS-2016-36
Wageningen University and Research Centre
Laboratory of Geo-Information Science and Remote Sensing

Abstract

Forest inventories are mainly based on satellite data for monitoring changes and management applications. The latest developments in Unmanned Aerial Vehicles (UAVs) allow rapid acquisition of very-high resolution (VHR) data, that could enhance forest inventories with information at individual tree level. This study showed that it is possible to extract top of canopy (TOC) individual tree crown (ITC) shape parameters based on UAV acquired data, in a dense tropical forest. Field survey measurements and terrestrial laser scanning (TLS) data were used for validation.

To overcome geo-referencing inaccuracies of multi-source data a semi-automated co-registration was proposed. The point clouds derived from photogrammetric processing of airborne VHR images and TLS, and field survey measurements, were successfully co-registered based on: point clouds to meshes generation, transformation matrices derived by rough and fine alignment based on the iterative closest point (ICP) algorithm and trunks mapping. A region growing method was followed for the ITC delineation approach with an accuracy of 69.2%, taking advantage of the availability of the VHR orthomosaic and the digital surface model (DSM). Based on a DSM filtering and local maxima (LM) approach the treetops were detected and used as seeds for the geographical object-based image analysis (GEOBIA) on the region growing method. The delineated ITC polygons were used for the segmentation of the point clouds.

A hemi-ellipsoid model approach was proposed, and proved successful for fitting the point cloud segments and extracting the upper crown height and width, and the crown curvature. The results showed that the hemi-ellipsoid fitting could describe adequately 54.1% of the segments, while the erroneous ITC delineation (over- or under-segmentation) is the main reason for model fitting failure. Photogrammetric point clouds (PPCs) are an approximation of the real tree crown and the hemi-ellipsoid is a simplified way for modelling trees, both influencing the success of this approach. The statistical assessment of crown shape parameters for species delineation, in order to validate consistency, showed that trees of the species *Tristaniopsis whiteana* and *Dehaasia caesia Bl.* (Pelawan, Perawas in local name) clustered when tested in paired comparison with other species. However, it is not feasible to discriminate between all different species of the tropical forest solely based on these parameters. Crown curvature is the most appropriate parameter for species discrimination compared to crown height and width.

Overall, the crown shape parameters are useful for management and monitoring applications on forest inventories. Specifically, for forests undergoing development, detection of disturbances, growth trends, thinning operations, forest fire and disease spread simulations can take advantage of shape parameters. An effort is made within this report on the documentation of the possible capabilities and limitations of these parameters.

Keywords: co-registration, hemi-ellipsoid fitting, crown shape parameters, Unmanned Aerial Vehicles, 3D point clouds, tropical forests, geographical object-based image analysis

Preface

Exploring new sensing methods, low cost alternatives for faster acquisition of data, instead of traditional satellite or alternative aerial methods always interested me. Centurion said *Elevatis nihil celatur* which translates to *To those high up, nothing is concealed* although the purpose was different the idea is the same. More information, leads to advantages to those with the information. I think right now we are in the beginning of a new era where UAVs, and in general unmanned vehicles, can be seen as a valuable tool for exploration for the benefit of our planet. In some cases, they can be used complementary with other methods or as alternatives where other methods are not applicable.

During this thesis I learned a lot, improving my scientific and practical skills in order to find appropriate ways to solve my research questions. Some of the research questions were solved by thinking out of the box, and with a simplistic approach, while for other more advanced methods were used. I learned that a failure is more common than a success but in both cases there is always something to learn from.

This thesis would not be possible unless my supervisors trusted me with this topic. Your guidance and patience had a major impact on my studying curve in all phases of this thesis. Specially, I am grateful for our frequent meetings where your almost “parental” advices on how to work efficiently, with a schedule, and of course scientific guidance helped me reach my goals. Juha’s algorithmic advice on how to calculate precisely the necessary time for solving an unknown problem is something I will always keep in mind. Sometimes when things do not work out, motivation goes down as well but this is all part of the research process, I am lucky you were always there for me.

I would also like to thank my parents for financial and moral support in the pursue of this second master, and for having me as a priority besides difficulties. Special thanks to my friend Penelope Kourkouli for her recommendations and time spend for reviewing this report. My MGI friends for making me feel like home in the thesis room daily with coffee and lunch breaks, and the (sometimes longer than supposed to) table tennis games. Last but not least, I would like to thank my partner for making winter days brighter, life happier in total, and managing to find time for reviewing this report.

Wageningen, December 2016

Table of Contents

List of Abbreviations

2D Two Dimensional

3D Three Dimensional

ALS Airborne Laser Scanning/Scanner

CHM Canopy Height Model

CIFOR Center for International Forestry Research

CMM Canopy Maxima Model

DBH Diameter at Breast Height

DGNSS Differential Global Navigation Satellite System

DSM Digital Surface Model

GEOBIA Geospatial Object Based Image Analysis

GNSS Global Navigation Satellite System

GPS Global Positioning System

ICP Iterative Closest Point

ITC Individual Tree Crown

LiDAR Light Detection and Ranging

LM Local Maxima

NFI National Forest Inventories

OBIA Object Based Image Analysis

PPC Photogrammetric Point Cloud

REDD+ Reducing Emissions from Deforestation and Forest Degradation

RS Remote Sensing

RQ Research Question

TOC Top of Canopy

TLS Terrestrial Laser Scanning/Scanner

UAS Unmanned Aerial System

UAV Unmanned Aerial Vehicle

VHR Very High Resolution

1. Introduction

1.1. Context and Background

1.1.1. Importance of forests

Forests are of major importance considering their ecological and economical value. Forests preserve soil, water, carbon, and biodiversity while nearly one third of earth's population rely on forests resources (FAO, 2014). Globally forests face natural and human-driven disasters such as fires, diseases, illegal logging, and converting forest areas to agricultural or other land use due to population growth. These disasters, and changes in land use result to deforestation, and forest degradation. For the reduction of emissions related to deforestation and forest degradation programs like REDD+ were initialized in order to motivate less developed countries towards sustainable forest management. Since 2005, estimations show that globally deforestation rate was reduced, although still tropical forests are subjected to degradation and deforestation which accounts for 12-20% of the global greenhouse gas emissions that contribute to climate change (FAO, 2014; Van der Werf et al., 2009). In Southern Asia between 1990-2005 the annual deforestation rate actually increased emphasizing the need for consistent monitoring applications (Sodhi et al., 2010).

1.1.2. Monitoring forests

The national forest inventories (NFI) are using remote sensing (RS) techniques with sample-based procedures in order to acquire information about forest resources (Koch, 2013; McRoberts and Tomppo, 2007). RS techniques are used for mapping forest area and volume, by deploying optical, radar, and laser sensors in platforms of different elevation (ground, aerial, and satellite) (Fagan and Defries, 2009). Global estimations accuracy rely on the quality of data acquisition and depend on statistical errors which are causing uncertainties in monitoring trends in forest areas (Grainger, 2008). By reducing the uncertainty, and increasing the accuracy of forest volume and area measurements, programs like REDD+ can monitor efficiently the progress of countries involved (Herold and Schiller, 2009).

The more information we can provide about the structure of the forested area the better we can understand forest growth trends, allometric relationships, biomass volume variations, and use as additional input in species classification. Structural parameters of the tree's crown can facilitate forest management applications, which could result in higher accuracy of forest mapping and support the regional and national forest inventories.

Most applications rely on satellite missions such as MODIS, and Landsat for monitoring forests in a coarse pixel size (Hansen et al., 2009) but the last two decades there is an increasing interest for fine scale applications. For the acquisition of VHR data both satellites, and airborne vehicles are used; such as UAVs. UAVs that are capable to carry on-board sensors, and to acquire VHR data for retrieving structural and spectral information of the forests mostly are referred as Unmanned Aerial Systems (UAS). Autonomous UAVs are considered as low-cost compared to manned aerial systems (Eisenbeiß, 2009). The technological advances made this possible with the miniaturization of metric and non-metric cameras, and GNSS systems (Colomina et al., 2008).

Koch et al., (2008) refer to the available techniques for forest monitoring and emphasize the successful use of light detection and ranging (LiDAR) techniques for regional inventory level. Due to operational restrictions of the TLS, and the need for larger area coverage, most studies refer to point cloud data collected by airborne laser scanning (ALS), and combination with aerial high resolution images (Dalponte et al., 2012; Moffiet et al., 2005; Monnet and Mermin, 2014; Ørka and Dalponte, 2013; Orka et al., 2012). ALS and TLS are capable for accurate individual tree detection and segmentation in dense forests thus proven in several studies as the most accurate techniques for forest volume measurements. However, still are considered as the most data intensive, and operationally expensive techniques (Calders et al., 2015; Fagan and Defries, 2009).

Lately, the capabilities of photogrammetric point clouds (PPCs) acquired by UAVs, are explored and compared with the ALS point clouds. Reconstructing the three dimensional (3D) forest model with photogrammetric techniques, based on data derived from a UAV, is often a good alternative to satellite (models from VHR stereo pairs), and manned aerial systems depending on the study's accuracy requirements. The top of canopy, individual trees delineation performance, tree-species or tree-type distinguishing ability, and stems mapping are some of the applications where PPCs show comparable results with ALS point clouds (Fritz et al., 2013; Rosca, 2015; St-Onge et al., 2015). Both VHR optical, and laser data can provide tree-level information based on the individual or semi-individual tree crown (ITC) delineation approaches. As mentioned in Orka et al. (2012) an increase in classification accuracy can be achieved when different datasets are combined using the ITC delineation approach.

1.2. Problem Definition

The co-registration of multi-source data is a topic addressed in many studies since it is the only way to make valid comparison of datasets and perform further analysis. Finding the least time consuming and most accurate approach regarding the requirements of the study, is not always a straightforward task. Often, for data geo-referencing during field and aerial surveys the differential global navigation satellite systems (DGNSS) are used (Olofsson et al., 2008; Ørka and Dalponte, 2013).

Multi-source data might come with different coordinate systems. Although the different coordinate systems can be easily converted into the same system (*i.e.* WGS84) considering the geo-referencing procedure is accurate, in tropical forests there are conditions that can influence both the accuracy of the original geo-reference and the quality of the data. Some of these conditions are: signal attenuation of the GPS signal in ground measurements due to the dense forest canopy (Kaartinen et al., 2015), human induced errors in field survey measurements, occlusions on the LiDAR data, duplications in the photogrammetric point cloud (due to the reconstruction process) which are also expected to influence the co-registration process in this study.

In order to deal with geo-referencing errors in two dimensional (2D) data, transformations are quite common (*i.e.* image to image, image to map, based on gcp's orthorectification). However, there is no clear approach on performing spatial transformations in point clouds. Most point cloud matching algorithms come from the domain of computer vision, some require reference points (buildings, crossroads, gcp's etc.), in order to perform a fine registration (Armenakis et al., 2013) while some rely on detecting three dimensional self-similarities within the point clouds (Huang and You, 2012). In tropical forests it is not as easy to find recognizable features that could be used as reference compared with urban areas. Since the source of the point clouds is different (photogrammetric and TLS) there will be differences in the point spatial distribution and density which can cause confusion in automated matching algorithms. Another issue is that some of these algorithms are not open source, therefore cannot be further tested.

Besides the co-registration, the segmentation of individual trees within the point clouds can also be affected by the way branches merge between neighboring trees in dense tropical forests. Many studies refer to object based image analysis (OBIA) for ITC delineation when data such as VHR orthomosaic and DSM are available. OBIA accounts for several factors (textural, spectral, spatial etc.) thus it is estimated that crowns delineated with this approach are useful for the point cloud segmentation.

The study of Onge et al. (2015) showed that ITC delineation and tree species classification accuracy is similar between photogrammetric point clouds (combining 3D shape and spectral properties), and ALS point clouds. However, this approach was successful on the classification of four species, thus the results could differ when having more species or/and without the use of spectral information. Moreover, several approaches exist to derive crown shape parameters from ALS point clouds, by modelling the entire tree crown (Holmgren and Persson, 2004), however research is limited on crown shape parameter extraction from photogrammetric point clouds.

The appropriate modelling approach is related to the selection of parameters that are expected to be extracted thus these parameters should be useful for forest management and monitoring applications. In order to identify these parameters, it is essential to review the input parameters used in simulation applications for forest management. For example, in BehavePlus (fire behaviour modelling system) among the other parameters the crown width and height are of importance (Andrews, 2009). In the recent research of Pimont et al. (2016) the following parameters prove to be valuable: the diameter at breast height (DBH), crown diameter, crown height, and crown geometry (ratio of maximum diameters to heights). These parameters are valuable for modelling purposes on thinning, pruning, clearing and prescribed burning. Also are identified as important for forest fire modelling, biomass and other canopy structure variables through allometric equations (Chen and Qi, 2013; Keane et al., 2012; Reinhardt et al., 2006).

1.3. Research Objectives and Research Questions

The main objective of this study is to propose a methodology for the extraction of individual tree crown shape parameters in tropical forests based on a photogrammetric point cloud. A second objective is to investigate the consistency of these parameters, by performing a statistical analysis on correlation of species based on these parameters. Furthermore, a review will be done for potential usage of these parameters regarding forest inventories. In order to derive the ITC point clouds and link them with the field survey records a co-registration approach of multi-source data is mandatory. In order to fulfil these objectives, three separate but sequential research questions have been formulated:

RQ 1. Can a semi-automated methodology be applied for co-registration of UAV, TLS, and field survey data?

RQ 1.1. How to co-register point clouds coming from different sources?

RQ 1.2 How to co-register point clouds with field survey measurements?

RQ 2. How can the crown shape parameters be extracted from the point clouds?

RQ 2.1. How to derive individual tree point clouds?

RQ 2.2. What model fitting approach to use for the crown shape parameters extraction?

RQ 3. Are crown shape parameters consistent and what are potential applications for these parameters?

1.4. Outline

The second chapter, reviews the available research methods and techniques, indicating the close relationship of RS and forestry. It is essential to investigate how previous studies addressed similar challenges, and whether these solutions are applicable in this study. The third chapter starts with an introduction to the study area and the available dataset, and presenting the methodology followed from pre-processing up to the statistical analysis. To allow coherence in chapter three, the pre-processing results are also included. The fourth chapter, consists of the results of the processing, towards answering the second and third research question. The fifth chapter consists of a detailed discussion and evaluation of the methodology. The sixth chapter contains the conclusions and recommendations for future studies in order to facilitate similar topics.

2. Literature Review

2.1. Data Co-Registration

Depending on the quality of the datasets and the requirements of the study there are manual, automated and semi-automated techniques. Hauglin et al. (2014) showed that it is possible to co-register different datasets manually based on the coordinates of single trees and visual interpretation, however this approach is rather time consuming and not applicable for an operational scale. An algorithm was proposed by Olofsson et al. (2008) for automated co-registration of field survey data and remotely sensed data based on the canopy height model (CHM) and single trees detection. This method requires a high point density, and very accurate measurements during the field survey regarding the location of single trees (measured with GNSS).

The values of diameter, instead of tree height has also been studied for co-registration purposes (Monnet and Mermin, 2014). In other studies, algorithms were developed by combining GPS measurements and topographic surveying (Pascual et al., 2013). Dorigo et al. (2010) used the angle count sampling method related with the DBH. Advanced co-registration approaches between point clouds are based on the ICP algorithm (Yu et al., 2006), 3D self-similarity parameters (Huang and You, 2012) and plane correspondence (Armenakis et al., 2013). Hausdorff distance algorithm was also used for matching ground trees with TLS trees (Beauchemin et al., 1998).

During the data collection of this study, the location of individual trees was determined by the fieldwork teams based on a local grid (local coordinate system (0,0)) by measuring the x, y distance from origin, along with other survey parameters (species registration, DBH and height measurements). For the TLS-based data global, project, and local coordinates (different from survey data) are available deriving from the GPS device mounted on the TLS. The UAV-based data are geo-referenced based on the inertial navigation system (INS-GPS, global coordinates) of the hyperspectral mapping system (HYMSY). One of the objectives of this study is to develop a semi-automated methodology for data co-registration regarding the photogrammetric and TLS point clouds, and field survey data. Treating the point clouds as a surface through mesh reconstruction and using algorithms appropriate for matching point clouds are some of the techniques that will be further investigated. A point of attention is to ensure that spatial resolution remains the same within the different data, in order to do comparisons and estimate the co-registration accuracy. The UAV INS-GPS measurements are treated as the most reliable source, because the signal is not attenuated by the tree's canopy and hence will be used as reference in order to correct the TLS-based and field survey data.

2.2. Treetop Detection and Individual Tree Crown Delineation

According to Wang et al. (2004) ITC delineation is considered as a high-level vision problem, and four different types of algorithms have been developed for automatic delineation: local maxima (LM)-based, contour-based, template-matching-based, and 3D model-based methods. There are several stages for the ITC delineation, the main are: detecting the treetops by geometry and/or radiometry, detecting the crown boundaries, and performing a segmentation method.

Several studies refer to the LM approach for treetop detection (Holmgren and Persson, 2004; Persson et al., 2002; Popescu and Wynne, 2004; Suratno et al., 2009; Tiede et al., 2005). Regarding multispectral/hyperspectral imagery (satellite or aerial), Brandtberg and Walter (1998) used an edge detection approach for mapping the crown boundaries (gradient-based), whereas Gougeon and Leckie (2006) used a valley-following method (intensity-based). Regarding LiDAR data, crowns are delineated either from a smoothed CHM after finding the local maxima or directly from segmenting the point cloud. Zhang et al. (2015) refer to the tree climbing algorithm for treetop detection and to the donut expanding and sliding algorithm for tree boundary extraction, using LiDAR data. The watershed segmentation approach is frequently used according to the literature review for both datasets (LiDAR and hyperspectral images) (Alonzo et al., 2014; Heurich, 2008; Holopainen et al., 2013; Hyyppa et al., 2000; Latifi et al., 2015; Reitberger et al., 2009, 2008; Wang et al., 2004; Xiao, 2012). Recent studies refer to the 3D segmentation as a promising approach in forest structural parameters, capable of detecting smaller trees (Jakubowski et al., 2013; Reitberger et al., 2009; Yao et al., 2012).

Moreover, object-based image analysis can be used for individual tree detection because of the availability of VHR orthomosaics, and the powerful algorithms of eCognition software (Blaschke, 2010; Jakubowski et al., 2013). Objects are clusters of pixels with similar spectral, spatial, morphological, contextual and temporal properties. Compared to image-based analysis, these multidimensional properties of the objects are an advantage (Kumar, 2006). As recommended by the minor thesis of Nurhayati (Nurhayati, 2015), VHR orthomosaics can be segmented based on the OBIA approach in order to delineate the tree crowns. In this study, OBIA will be referred as geospatial object based image analysis (GEOBIA) in order to acknowledge the geographic related discipline, as the term OBIA is used broadly in many disciplines. According to (Blaschke et al., 2014) GEOBIA is based on the concept of all the previous segmentation methods (edge-detection, feature extraction), while offers a good potential when spectral properties are not unique by using distinct shape or neighborhood relations, texture, context and pattern mining, semantics and knowledge integration.

The reason that so many different methods are proposed by literature is that tree crowns in tropical forests are irregular and relatively complex, while advances in technology provide more alternatives in methods (development of powerful software and acquisition of high resolution data). Once the ITC delineation is achieved, it can be used for the photogrammetric and TLS point

clouds segmentation. Then an inventory of each tree's field survey data, photogrammetric and TLS point cloud segment can be created.

2.3. Model Fitting and Crown Shape Parameters Extraction

A model is an abstract and partial representation of some aspect or aspects of the world that can be manipulated to analyse the past, define the present, and to consider possibilities of the future (Couclelis, 2000). The art of modelling lies in making the right decisions on the aspects of the real world to include. In order to do that the following must be specified: a) the goal of the model, b) the available data, c) the skills of the modellers (Ligtenberg, 2016).

Model fitting of individual trees from point clouds can be done by various methods, generally including segmentation algorithms followed by geometric fitting of tree attributes. The following geometric fitting methods for tree reconstruction are frequently used: 3D voxel-space and fitting cylinders (Gorte and Pfeifer, 2004), neighbor-relations and locally connected surface patches (Raumonen et al., 2013), vector model of individual trees for feature extraction (Pyysalo and Hyyppä, 2002), 3D cylinder reconstruction (Burt et al., 2013), alpha shapes (Holmgren et al., 2008), wrapped surface reconstruction and locally applied regression model (Kato et al., 2009), implicit surface reconstruction through iso-surfaces (Kato et al., 2007), and ellipsoid modelling (Shahzad et al., 2015; Sheng et al., 2001).

According to literature the basic structural parameters for forest management applications suitable for tree species discrimination are the crown length, crown width, DBH, and tree height (Korpela et al., 2007; Morsdorf et al., 2004; Pratihast, 2010; Vaccari, 2013; Zawawi et al., 2015; Zhang et al., 2015). The majority of the previous studies refer to urban areas or small patches of trees, but for tropical forests it is not certain how the segmentation and model fitting algorithms will perform. For the purposes of this study the crown length and width, and curvature (concavity; upward or downward) will be extracted.

3. Methodology

3.1. Study Area

The study area is located nearby Mentaya river in the peat swamp forests of Central Kalimantan province, Indonesia (Figure 3). The climate in this area is characterized as tropical rainforest with precipitation rates of 2.776 – 3.393 mm per year. The rivers in the area play an important role as transportation paths.

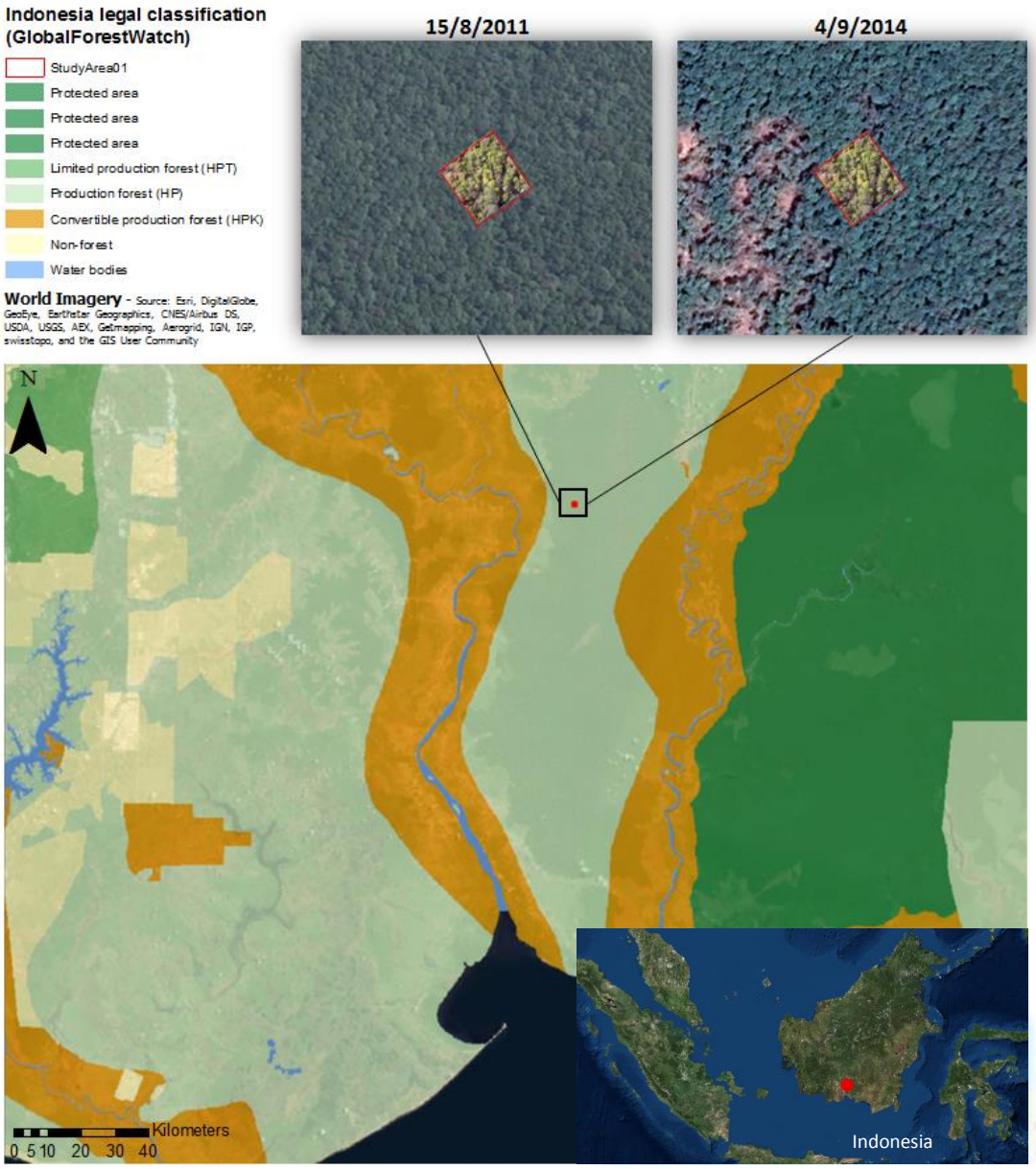

Figure 1. Map of the study area, Central Kalimantan Indonesia.

In Central Kalimantan, approximately 2/3 of the area is covered by forest and the main industries include palm oil plantations, timber plantations and coal mining. It is the 3rd largest province of Indonesia and the palm oil sector in this area contributes 25% in the provincial GDP (Report of Central Kalimantan and GGGI, 2015). The study area is classified as a production forest (HP) based on the legal classification, which means that it is a forest area designated primarily for production of wood, fiber, bio-energy and/or non-wood forest products (FAO, 2010). The most valuable trees are harvested and these changes can easily be detected by satellite images throughout the years but only in a coarse scale with no individual tree information.

In August 2014, a fieldwork took place under the framework of REDD+ program of Center for International Forestry Research (CIFOR). In total 14 different plots were measured based on three different data acquisition methods: a detailed field survey for biomass assessment (species identification, DBH, tree height, crown width measurement etc.), TLS surveys, and UAV flights. For the purposes of this research the first plot (Th01) is used as the study area. The plot area measures 40x40m and according to the CIFOR biomass inventory data it is an old logged forest and intensive logging operations are in progress. During the field survey for the inventory database the fieldwork teams registered trees with diameter larger than 10cm.

The dominant tree species are of the family group Non-Dicerecoptea (Table 4, Appendix 1). According to the field survey report, due to the growth of Terantang the forest looks relatively intact. For the inventory of plot's data, a total number of 227 trees were measured, containing 41 different species with the following 7 contributing to 50% of total trees according to the: Ubar (15.7%), Samak (8.9%), Pelawan (7.2%), Jingjiit (6.3%), (Meranti (5.8%), Terantang (4.5%) and Perawas (4.5%) referred by their local names.

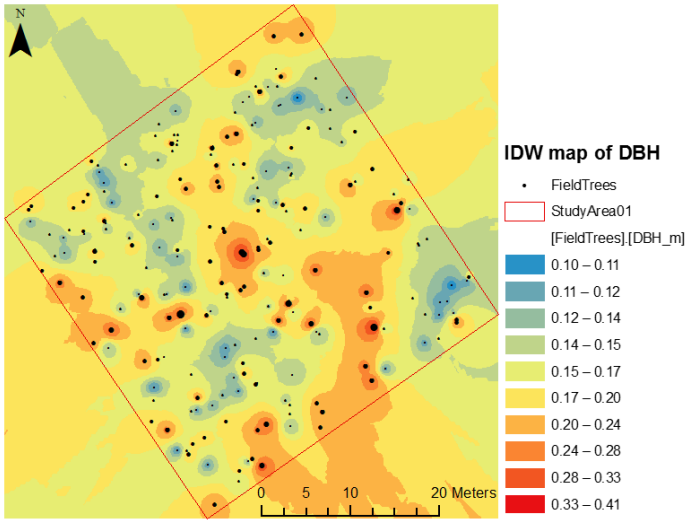

Figure 2. Inverse distance weights map of the trunk's DBH.

An inverse distance weighting map according to DBH from field measurements was prepared in order to identify possible clusters of bigger trunk trees which might be helpful in the future co-registration steps (Figure 4). This field map is geo-referenced because it was created after step RQ1.1, but it was included in this section for a better understanding of the study area.

3.2. Dataset

Unmanned Aerial Vehicle Derived Data

The WUR Unmanned Aerial Remote Sensing Facility (UARFS) has been using UAVs for different applications, including the forestry mapping campaign in Indonesia's peat swamp forests in the summer of 2014. Under the UARSF the HYMSY sensor was developed, consisting of a pushbroom spectrometer, a photogrammetric camera and a GPS-Inertial Navigation System (Suomalainen et al., 2014). During the campaign in Indonesia, the Okkie1 with HYMSY collected hyperspectral and VHR RGB images before and after logging activities. For the reconstruction of the PPC (Figure 5), the RGB orthomosaic and the digital surface model (Figure 3), the derived imagery (VHR RGB images down to 0.02m spatial resolution) was used. The top of the canopy (TOC) 3D model (Figure 4) can be generated by applying texture to the polygon mesh. The pre-processing methodology is further described in Chapter 3.4. Due to the dense tree coverage, trees are overlapping and the understory of the forest canopy cannot be fully reconstructed by these images, besides the areas within the images that have canopy gaps.

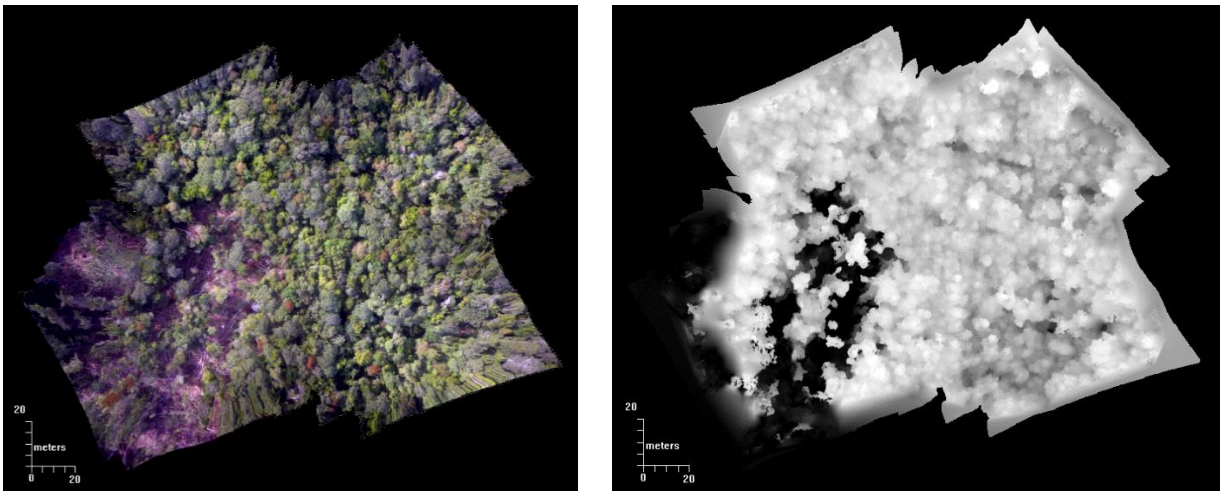

Figure 3. Left. The RGB Orthomosaic (0.043m resolution). Right. The Digital Surface Model (0.043m resolution).

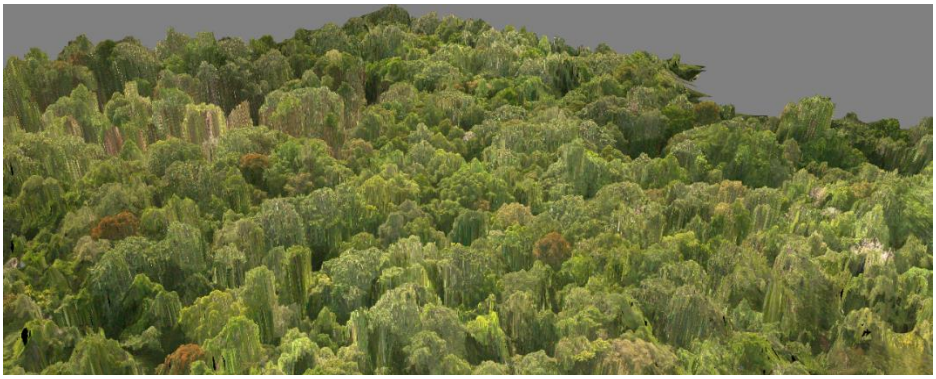
Figure 4. Textured 3D model of the forest canopy.

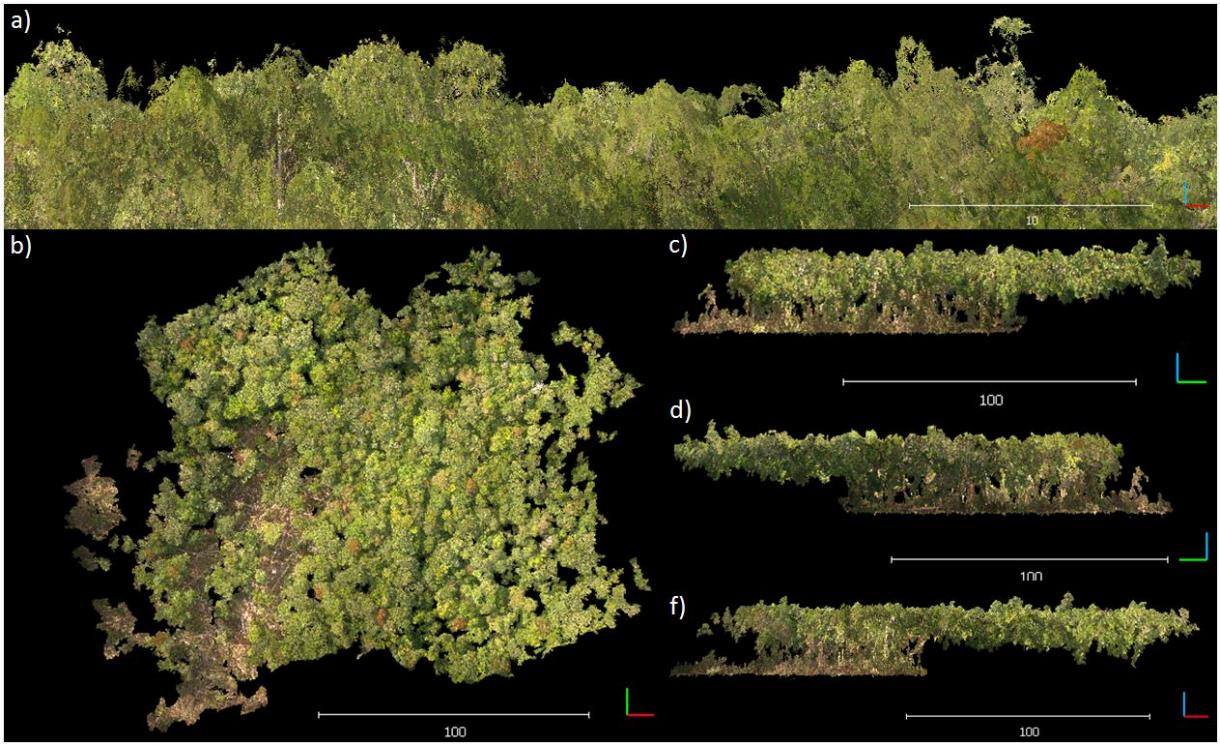

Figure 5. The PPC in different viewing angles, a) top of canopy, b) aerial, c) right side, d) left side and f) front side.

Terrestrial Laser Scanner Data

The Riegl VZ-400V is a full-waveform 3D TLS capable of providing data with accuracy of 5mm and a rate of 122.000 measurements per second (Riegl Laser Measurement Systems, 2014). Because of the density of the forest area multiple scans were performed and co-registered by reflectors that were installed within the plot. The main product of the TLS is the TLS point cloud (Figure 6). It will be used for the detection of the boundaries of the plot, the co-registration of the field survey data and for comparison with the PPC.

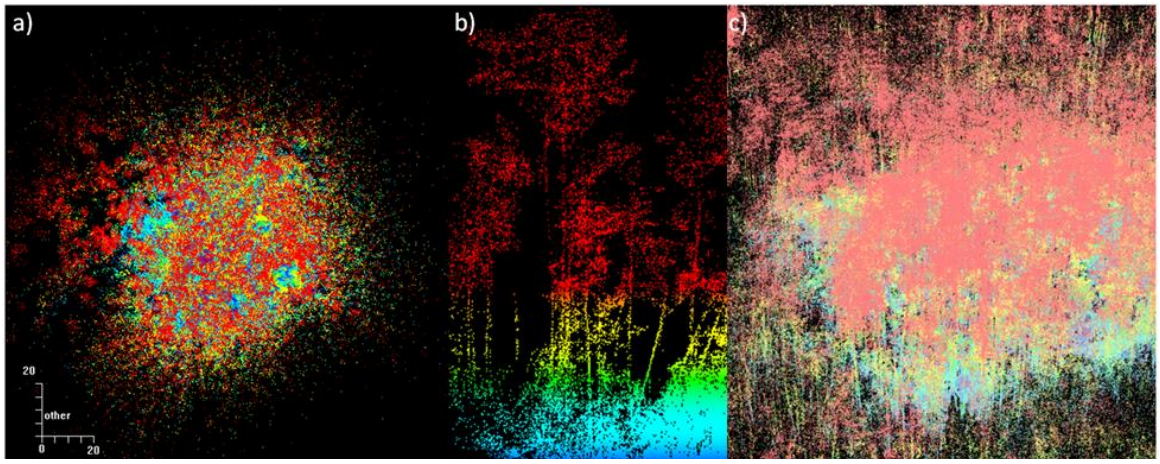

Figure 6. LiDAR point cloud from the Terrestrial Laser Scanning. a) aerial view, b) front side view, and c) 3D view.

Field Survey Data

The field survey is digitally stored in a form of excel sheets containing biomass inventory data. The position of the trees was measured in a local grid (x,y) reference system where the (0,0) position is the lower left corner of the plot. Each dot represents the identified trees and their relative positions which are also described within sub-plots (Figure 7). Apart from the (x,y) location for each tree, the field work teams collected further information such as: the tree's local name, botanical name, family group, circumference, and DBH.

Taking into account the x,y local coordinates a map of the field survey trees (as points) was created for further use and stored as shapefile (Figure 8) with the following attributes: Identity, Shape, Plot, Subplot, Local_name, Botanical_name, Family, DBH_cm, X_m, Y_m (Table 5, Appendix 1).

An overview of the available datasets of this study can be found in Table 1. The last row of the table refers to the coordinate system available for each dataset.

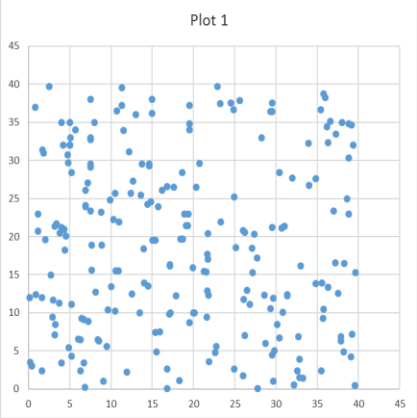

Figure 7. Field survey data map in excel.

Figure 8. Tree species map created in ArcMap.

Table 1. Overview of all dataset available (with and without pre-processing).

UAV data	TLS data	Field survey
DSM	DSM	Tree species
Photogrammetric point cloud	TLS Point Cloud	Circumference
Orthomosaic with 0.043 m resolution (RGB)	DBH	DBH
Raw VHR images		
GPS-INS Global coordinates	*Scan positions local, project and global coordinate system*	*X, Y local coordinates*

3.3. Methodology Overview

The flowchart in Figure 9 depicts an overview of the methodology towards answering the research questions. The proposed methodology is based on sequential steps, which are described in detail in Chapters 3.4 to 3.8. The data pre-processing is described in Chapters 3.4 to 3.6. An overview of the software packages used in this study, regarding each step, can be found in Table 2.

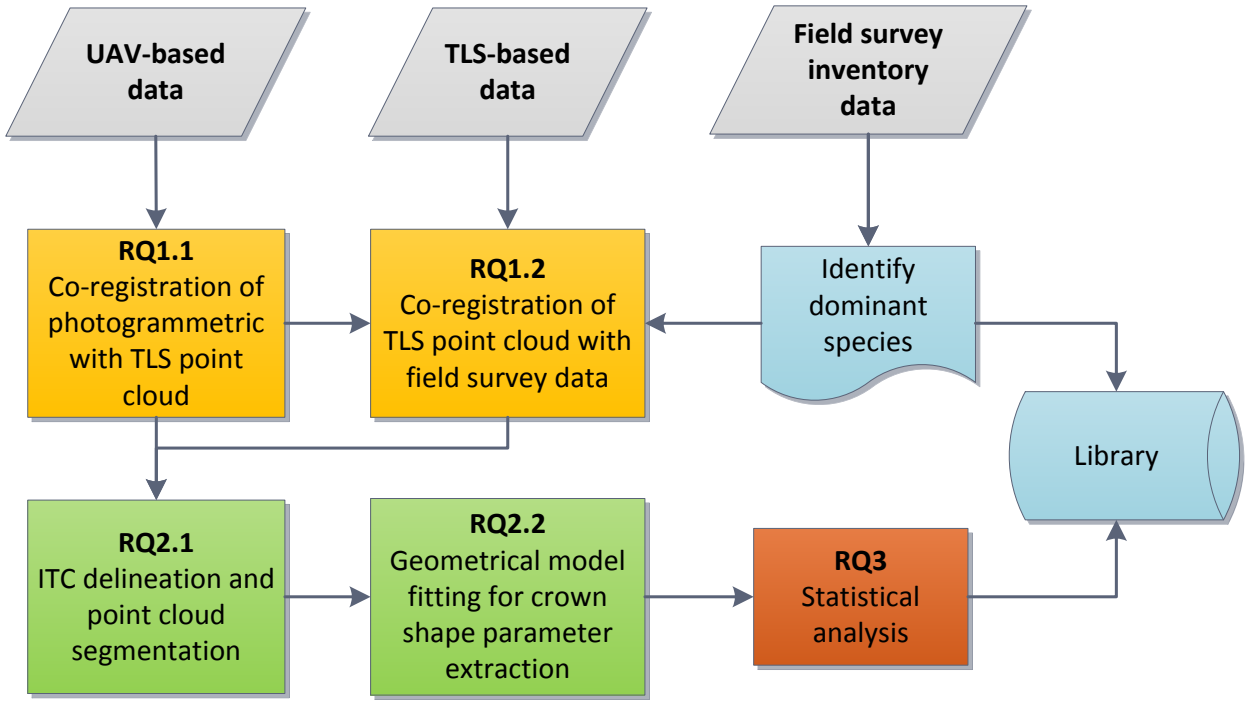

Figure 9. Flowchart of the methodology.

Table 2. An overview of the used software packages and the purpose of use.

Software	Usage	Step
ArcGIS	Vector, Raster GIS analysis, Create Maps	RQ1.2, RQ2.1
LAStools (ArcGIS toolbox)	Point Cloud analysis	Pre-processing
RiSCAN Pro	Point Cloud analysis	Pre-processing, RQ1.2
Cloud Compare	Point Cloud, Mesh analysis	RQ1.1, RQ1.2
eCognition	ITC delineation	RQ2.1
FUSION	Point Cloud analysis	RQ2.1
Matlab	Shape parameter fitting	RQ2.2
MS Excel	Create Inventory	RQ2.2, RQ3
R	Statistical analysis	RQ3
MS Word	Report Writing	
MS Visio	Flowcharts	

3.4. Pre – Processing

3.4.1. Derive Photogrammetric Point Cloud, Orthomosaic and DSM from UAV imagery

The PPC, is a product derived from the photogrammetric processing of the aerial images acquired by the UAV with the Panasonic DMC-GX1 (f=14mm) camera model. This procedure was done in Agisoft Photoscan Pro software and it includes steps as: the estimation of the quality of the images, alignment, build of sparse and dense point cloud, mesh, and texture. For further processing the output can be exported in different formats (LAS, ASCII, OBJ, DSM, XYZ points, PDF reports, etc.). The processing chain is entirely automated, and only the quality (high) and depth filtering (mild) parameters needed to be predefined for the reconstruction of the 3D model. For Plot Th01, 86 aerial images of a flying altitude of 69.3m with ground resolution 0.016m/pix and a coverage area of 0.03km^2 were used. The digital surface model has a point density of 902.874 points/m^2 and resolution of 0.03m/pix (Figure 10).

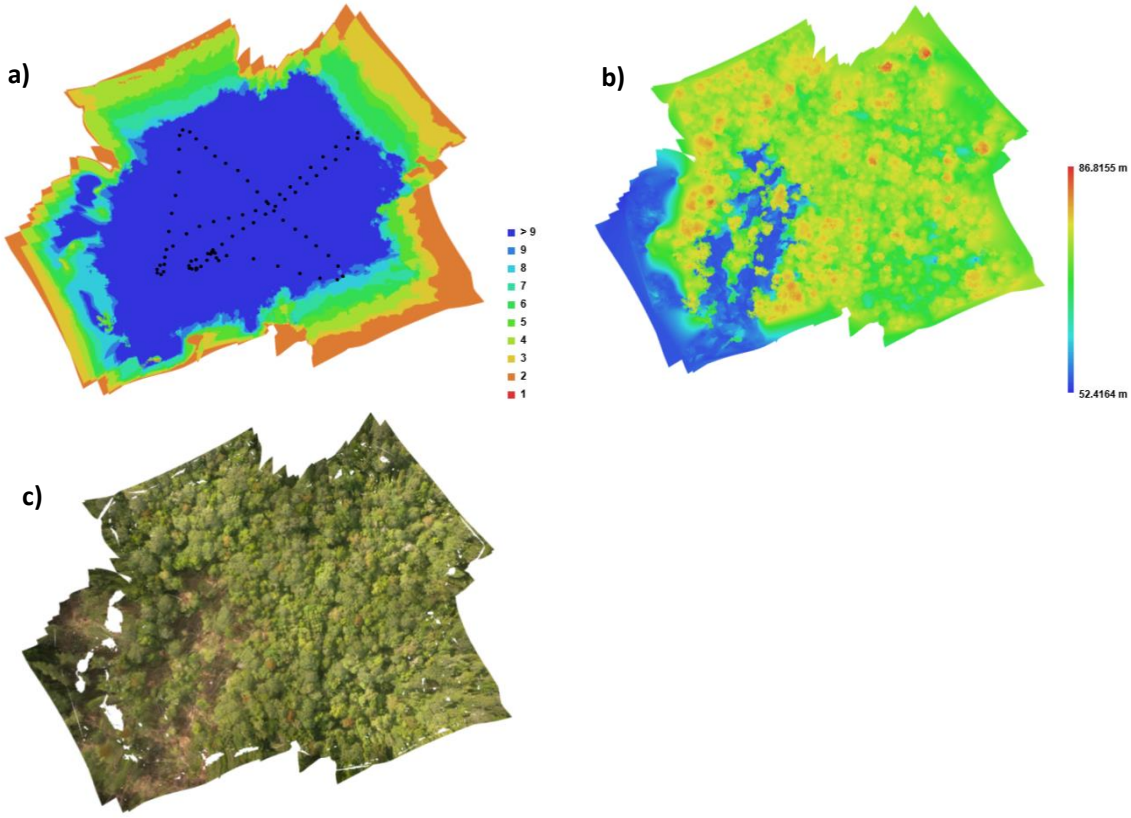

Figure 10. a) Camera locations and image overlap, b) Digital surface model and c) Orthomosaic.

3.4.2. Detect the Plot Boundaries on TLS point cloud

The raw data consists of multiple scan positions (13) each in Upward and Tilted direction. The detection of the plot boundaries was done by using the height filter in RiSCAN Pro software package, where at about 0.5m height the marking tape placed during fieldwork was visible (Figure 11). Creating a polyline based on this rectangular area corresponds to the plot boundaries extracted for further use. Working in the plot scale instead of the entire area covered by the TLS point cloud was done mostly for enabling the co-registration with the field survey data, but also for efficiency, data reduction and minimization of output storage requirements (entire area TLS point cloud is 9GB, while Plot Th01 is 4GB). Once the TLS point cloud is co-registered with the PPC, the boundaries can be retrieved for the orthomosaic and the DSM as well.

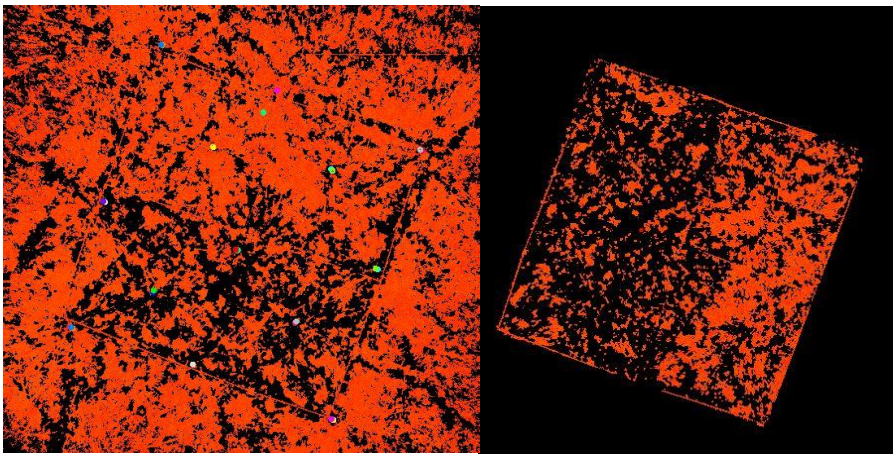

Figure 11. Extraction of plot boundaries from the TLS point cloud.

3.5. Semi-Automated Approach for co-registration of the UAV, TLS and field Survey Data

The first research question is part of the data pre-processing methodology, with the aim to propose a semi-automated approach for the co-registration of the data. For this purpose, the results of this first RQ will be directly presented after the methodology description and will not be included in the results on Chapter 4.

This step is vital when the conditions during data acquisition can interfere with the original georeference. The goal is to co-register UAV, TLS- and field –based data with the lowest possible error (RMSE) based on the PPC (reference data). Different software packages were used for this pre-processing step: Cloud Compare, ArcMap and RiSCAN Pro. This research question is split into two different steps, a) the co-registration of PPC with the TLS point cloud, and b) the co-registration of the 'corrected' TLS point cloud with field survey data.

3.5.1. Co-registration of Photogrammetric with TLS point cloud

Once the PPC and TLS point cloud are visualized an offset can be observed from the TLS point cloud possibly due to the attenuation of the GPS signal due to the dense forest canopy (Figure 12). An affine transformation based on the boundaries of the plots cannot be done in this stage as there is no way to identify the plot boundaries on the UAV data. The actual boundaries mismatch is depicted in Figure 13, in order to show the extent of the offset in x, y and z axis (note that the plot boundaries for the UAV data, were retrieved only after the co-registration). The PPC is used as reference (model data), for the geometric transformations in order to correct for the offset on the TLS point cloud.

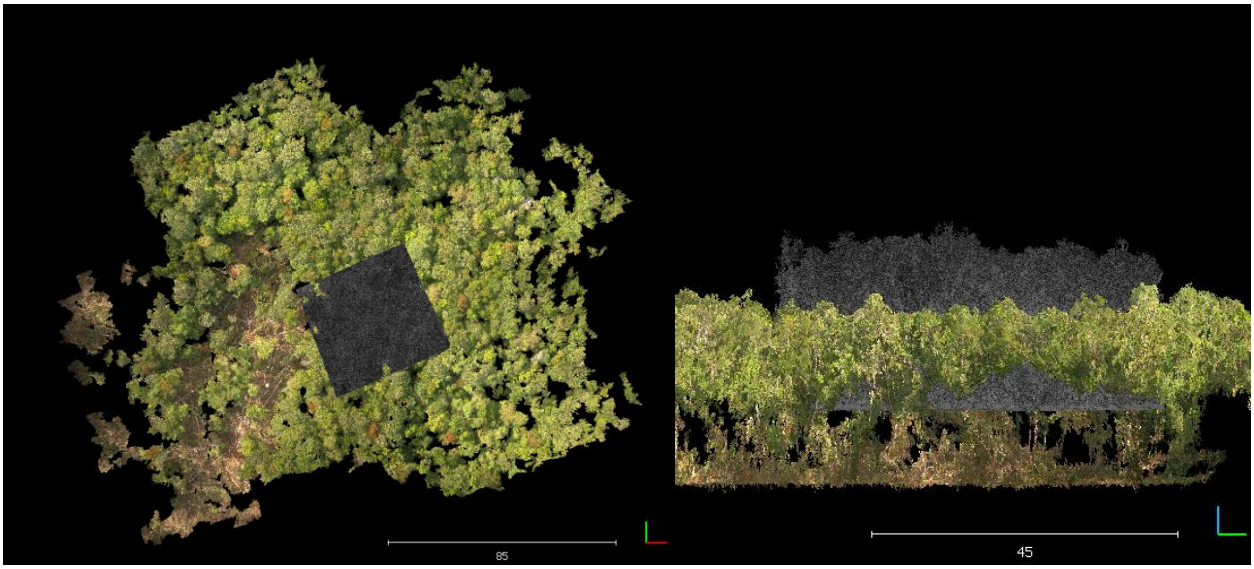

Figure 12. A visualization of the PPC of the entire extent & TLS point cloud, before alignment.

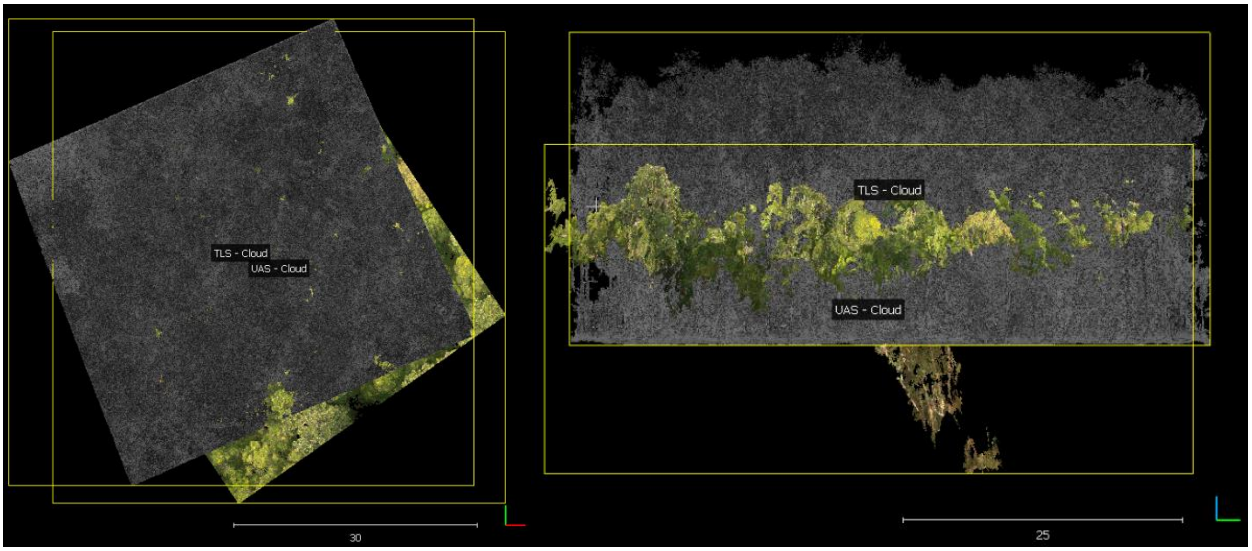

Figure 13. Left: PPC & TLS point cloud actual boundaries offset in X, Y axis. Right: Z axis offset. WGS 1984 UTM S49 projection system.

The approach for the co-registration of PPC and TLS point cloud is depicted in the flowchart in Figure 14. It is based on four processes starting with the generation of meshes from the point clouds, the rough alignment of the meshes, and the use of the transformation matrix of the meshes for the point cloud co-registration. Last, if the results of the rough alignment are not satisfactory a fine alignment can be performed based on the ICP algorithm. Each of the processes of the flowchart are further explained in the paragraphs below. The software used for this method is Cloud Compare.

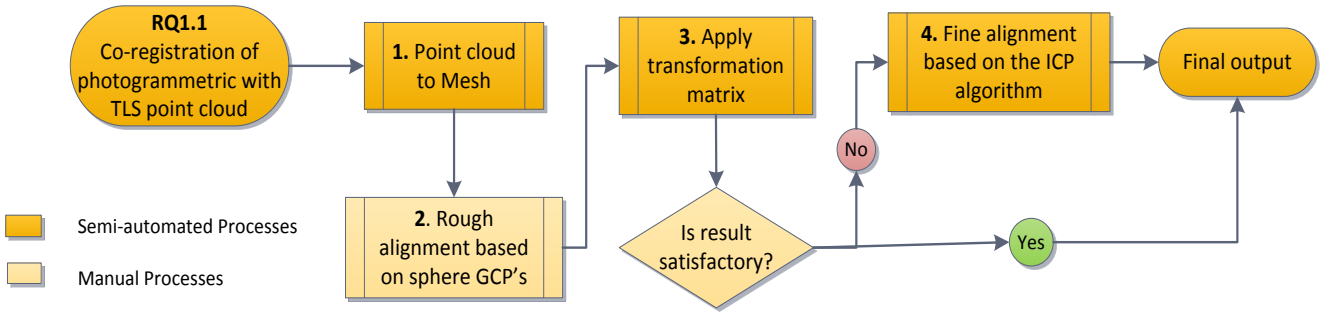

Figure 14. Flowchart of the procedure for co-registration of the point clouds.

(1) A triangular mesh is a point cloud with an associated topology, a collection of vertices, edges and faces that describe the shape of a 3D object. Generating and using the mesh permits the selection of relevant reference point pairs, something that could not be done in the point cloud directly.

(2) In this case, instead of point pairs “sphere” pairs are preferred, as the center of the spheres can be detected automatically by the software. This increases the speed and accuracy of the alignment process. When enough sphere pairs are selected the alignment of meshes can be performed, resulting to a transformation matrix which includes the RMSE of the procedure (Figure 15).

(3) For the spatial transformation of the TLS point cloud, the transformation matrix can be applied. This procedure results to a rough alignment. In case the result is not sufficient, (4) the ICP algorithm can be used for fine alignment of the meshes or directly of the point clouds. With the ICP algorithm a least square registration is possible, by converging to a local minimum (Besl and McKay, 1992).

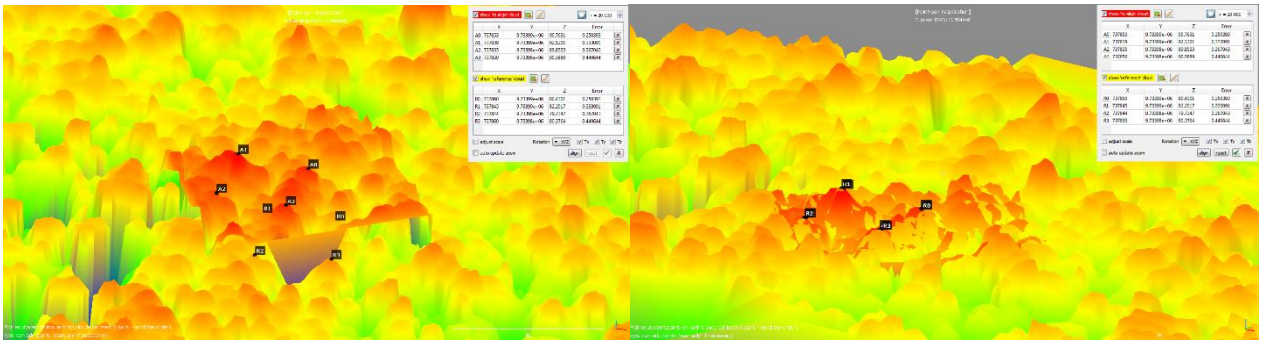

Figure 15. Sphere pairs selection for the alignment of the meshes.

3.5.2. Co-registration of TLS Point Cloud with Field Survey Data

Since the TLS point cloud is successfully co-registered with the PPC, this means that now the plot boundaries deriving from the TLS point cloud can be further used, to retrieve the plot boundaries in the UAV data and for the spatial transformation of the field survey data. A local to global coordinate transformation, based on the four corners of the plot boundaries, could be a sufficient solution, for the field survey data geo-referencing. As it was mentioned earlier the fieldwork teams acquired manual measurements of the tree locations based on a local grid (Chapter 3.2). It is expected that the manual measurements of the trees in the excel sheet could be relatively close to the actual tree location, but with a small offset, considering the limitations and difficulties of manual measurements in a dense tropical forest.

For this reason, the proposed methodology co-registers the data not only by using the boundaries, but each tree location of the field survey record is linked with a tree trunk location detected directly by the TLS point cloud. This is a very crucial step regarding the entire study because these trees will later be modelled and assessed for correlation between crown shape parameter and tree species, so misidentification of the trees/species could affect the results. In order to validate the final results, trees DBH derived from TLS point cloud and DBH from the field survey was correlated for several trees, along with visual assessment.

For the co-registration of the TLS point cloud with the field survey data the proposed methodology is depicted in Figure 16. This flowchart consists of five processes and the software packages used are Cloud Compare (process 1 to 4) and ArcGIS (process 5). Each process is explained in the paragraphs below.

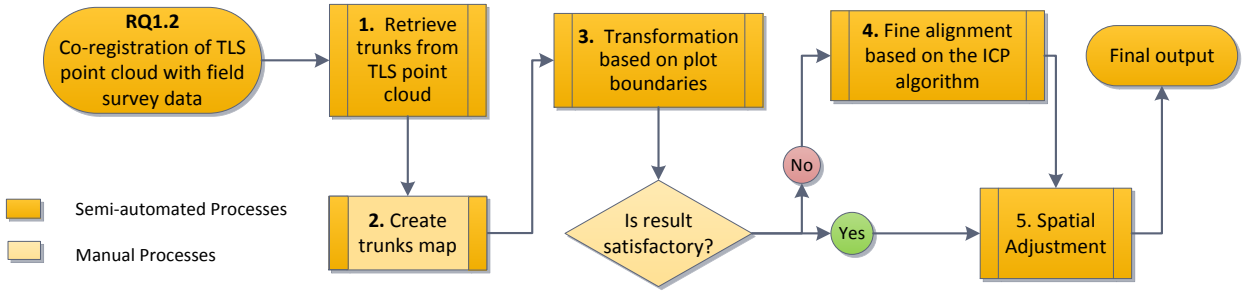

Figure 16. Flowchart of the methodology for RQ1.2.

(1) In order to retrieve the trunks from the TLS point cloud a cross section was created in about 1.2m – 1.4m height (approximately the same height used for deriving the DBH). The width of the cross section was selected to be of 20cm which is sufficient to identify cylindrical objects as the trunks, and to eliminate as much as possible of the noise (hidden branches and leaves in the understory in this height). Although, as it can be seen in Figure 17 there are still non-trunk objects (branches and leaves) that could interfere with the co-registration process.

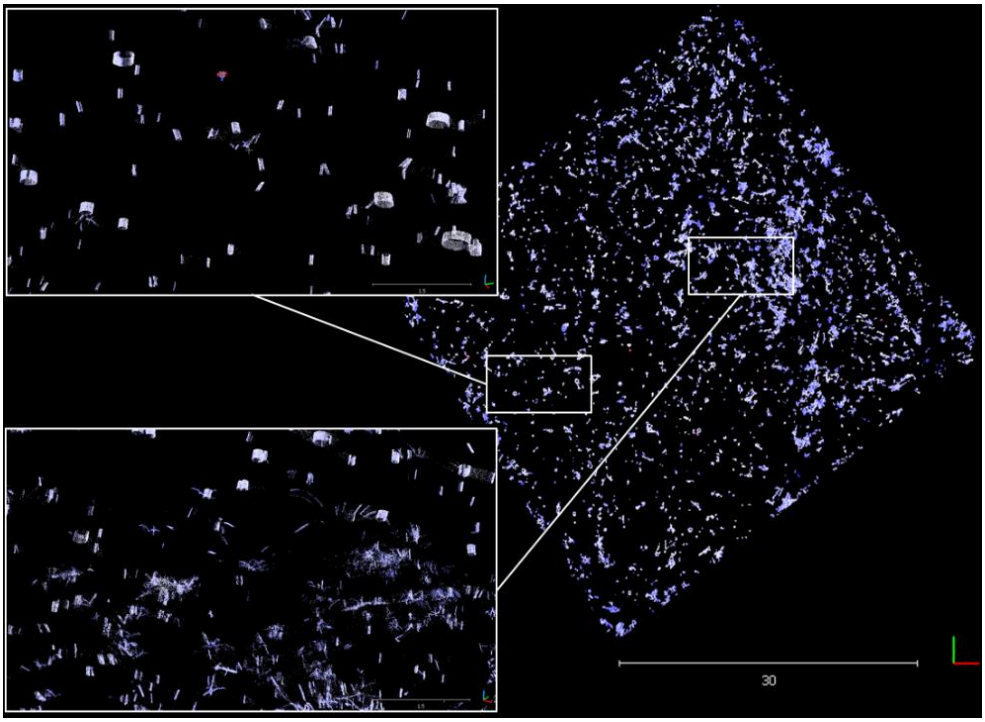

Figure 17. Trunks derived after cross section in the TLS point cloud.

(2) For the creation of a trunks map, the noise caused by non-trunk objects must be removed, and also each trunk must be assigned to a point location. A way to reduce the noise is by using the statistical outlier removal (SOR) and/or noise filter algorithm. These algorithms work by filtering out points that fall within a certain distance from their neighboring points. For this step the number of points to use for mean distance estimation was set to 5.0, and standard deviation multiplier threshold to 1.0 (max distance = average distance + nSigma*std.dev.) (Figure 18).

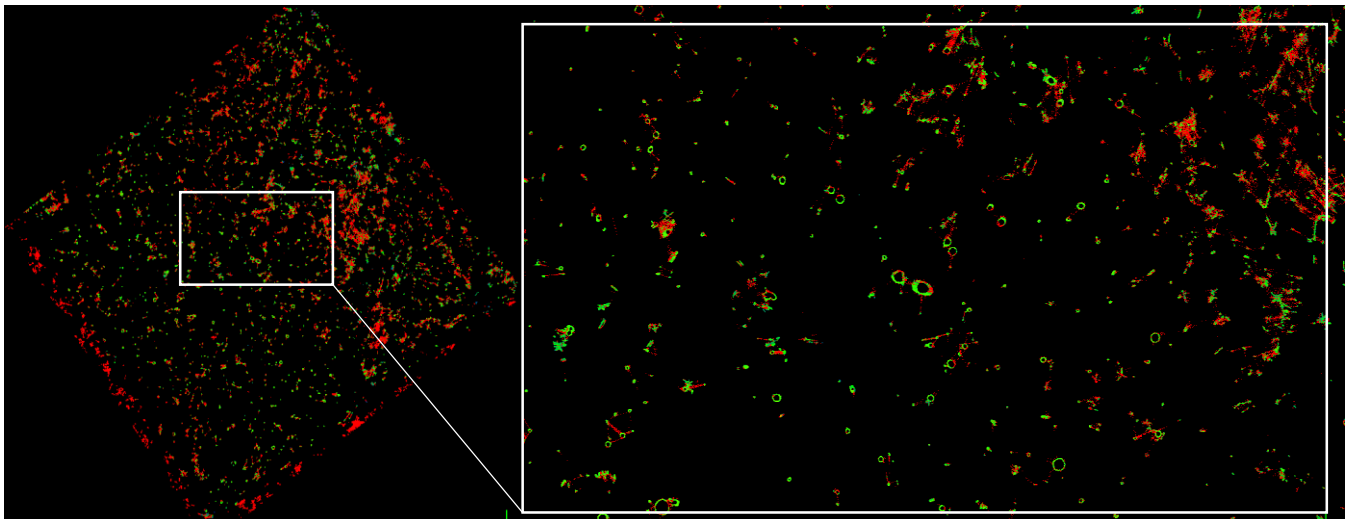

Figure 18. Trunks clean up after SOR algorithm (with red color are the points removed, green color are the remaining points).

Each trunk can be assigned manually or in an automated way as a tree point. Therefore, it is categorized somewhere between manual and semi-automated in the flowchart. In this case a tree point list was created manually (Figure 19). A way to automate this process, is to identify the trunks as cylindrical objects using minimum and maximum DBH threshold values, to avoid extreme outcomes.

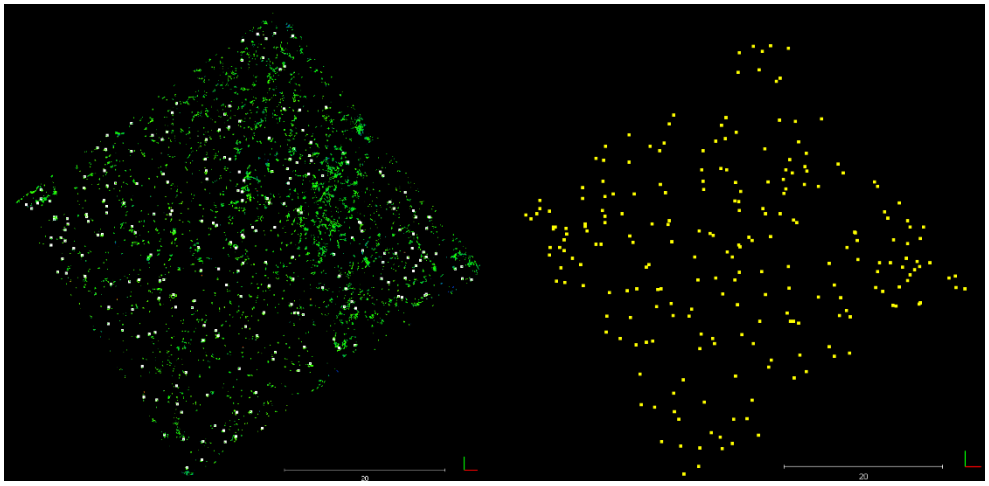

Figure 19. From trunks TLS point cloud to trunks point location map.

(3) An affine transformation of the field survey tree locations from local to global coordinates is performed based on the plot boundaries. We can visually assess the result of this transformation, compared to the trunk map that was created in the previous process (Figure 20. Left). Therefore, we can confirm that a transformation of the field survey data solely based on plot boundaries is not enough for the accurate co-registration.

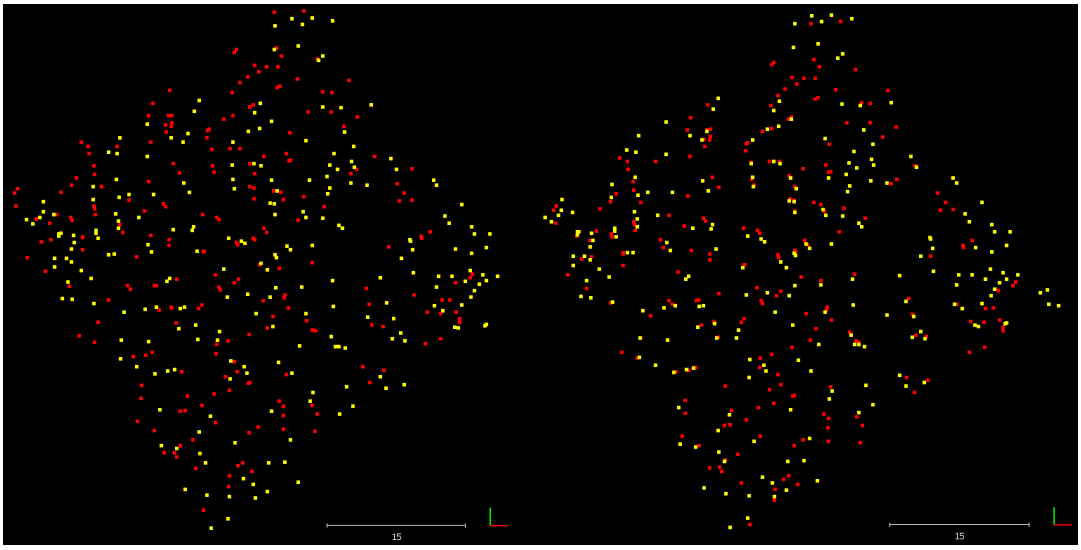

Figure 20. Left: Transformation based on boundaries. Right: Transformation based on ICP algorithm.

(4) In this case the ICP algorithm can be used to perform a fine alignment of the two different point entities (trunk points to field survey tree location points) (Figure 20. Right). The spatially transformed field survey tree location points, can be exported in a shapefile format. Since in Cloud Compare the shapefiles can only retain the location information of the points, and not the other attributes, one last adjustment is needed.

(5) This last process of this co-registration approach is to import the geo-referenced field survey tree points to ArcMap and transform the initial field survey file that contained the rest of information with the use of the spatial adjustment tool (Affine transformation).

Furthermore, in order to check the accuracy of the co-registration process, a Pearson correlation based on DBH values was performed, by comparing the field survey DBH measurements and TLS derived DBH measurements on eight randomly selected trees on the plot.

3.6. Assessment of the co-registered UAV-, TLS-, and field survey data

RQ1.1

In order to assess the accuracy of RQ1.1, the rigid transformation matrix used for the alignment of the original TLS point cloud, and the Final RMS are presented (Figure 21). It is a 4x4 matrix that represents rotation (3x3 matrix in green box) and translation values (a 3D vector in red box). The last row corresponds to the perspective projection of the camera plane and it is always 0, 0, 0, 1 in this case (Buss, 2003). The RMS corresponds to the square root of the mean value of the squared distances (Equation 1). This value represents the Euclidean (remaining) distance (d) between the sphere pairs after registration.

Final RMS: 0.354448

Transformation matrix

0.971	-0.237	0.017	2.998
0.237	0.971	-0.002	-9.822
-0.016	0.006	1.000	-9.691
0.000	0.000	0.000	1.000

Figure 21. Transformation matrix and RMS of the TLS and UAV point clouds rough co-registration.

$$RMS = \sqrt{\frac{1}{N}\sum_{i=1}^{N} di^2} \quad (1)$$

The Final RMS of the ICP algorithm performed in 50.000 points was 1.44 (Figure 41, Appendix 2), however in this case it did not improve the rough alignment result. This is mainly due the fact that many points in the TLS point cloud did not have any correspondence with points of the PPC. The RMS value derived from the rough alignment approach is relatively low (0.35m), and the result is considered as sufficient for the continuation to the next step. A visualization of the co-registration result can be found in Figure 22. The accurate detection of the plot boundaries in the UAV data (point cloud, orthomosaic, DSM) is now feasible and very important, for the step RQ2.

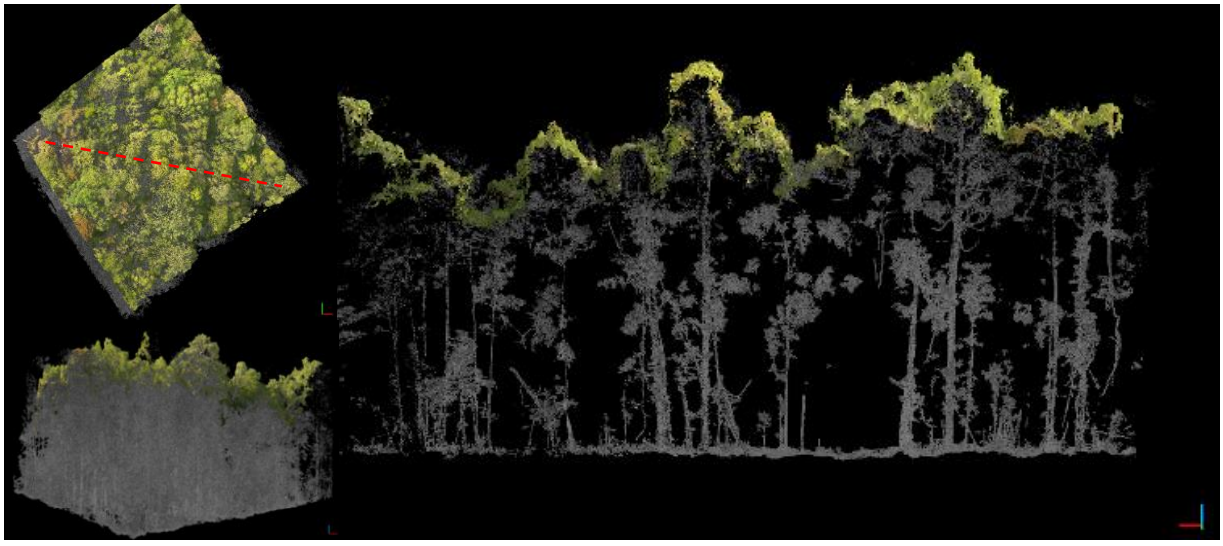

Figure 22. The co-registered Point Clouds. Left: view from above and side. Right: Cross section view (Plot Th01).

RQ1.2

As previously mentioned, in order to assess the accuracy of RQ1.2, the rigid transformation matrix is presented. The final RMS of the ICP co-registration (Figure 23) represents the Euclidean distance between each point of the not aligned cloud and its nearest neighbor in the reference cloud, and is computed based on the 226 points. The error of 1.3m could be attributed to the presence of no corresponding trees in the field survey, for some of the TLS derived trunk points (not all trees were mapped in the field survey tree points).

Final RMS: 1.30103 (computed on 226 points)

Transformation matrix

0.951	0.006	-0.167	3.199
-0.044	0.940	-0.217	7.585
0.161	0.221	0.926	26.337
0.000	0.000	0.000	1.000

Figure 23. Transformation matrix and RMS of field survey tree location points and trunks location points co-registration.

The result of ICP algorithm in the co-registration after visual inspection (Figure 24), is considered as acceptable as most of the field survey tree points show sufficient overlap with the trunks point location on the TLS point cloud. Based on the proximity, for some field survey trees with no overlapping trunks, we assume that the closest trunk is the one matching.

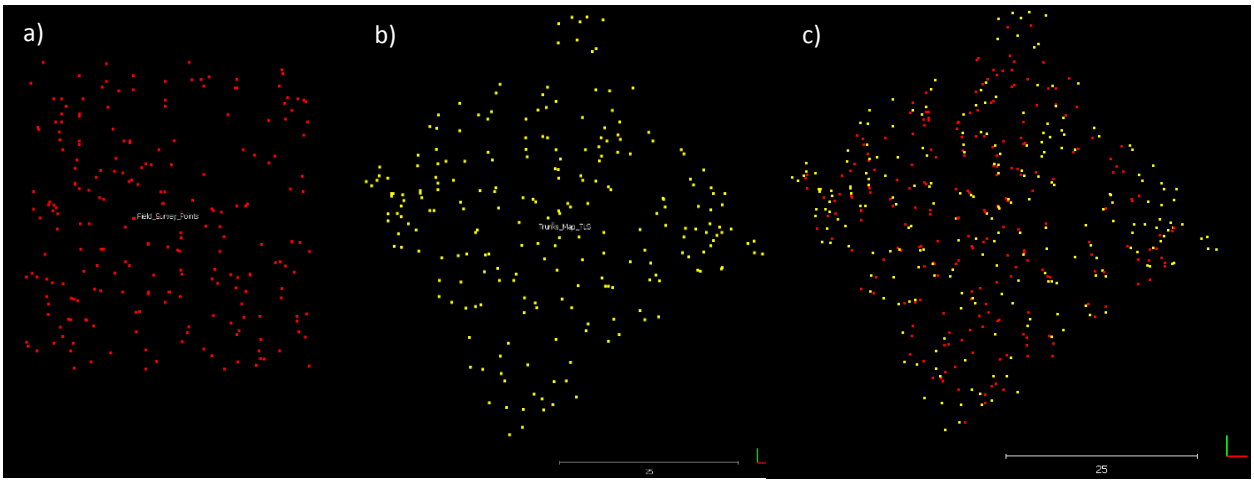

Figure 24. a) Field survey tree locations before transformation, b) Trunks map created by the TLS point cloud, c) The final result of co-registration of trunk points (yellow) to field survey tree points (red).

According to the correlation results of DBH between field and TLS measurements, a match of greater than 95% is estimated based on eight random samples. Therefore, apart from the visual interpretation of the results, we can conclude that the co-registration was successful as indicated by the DBH correlation (Appendix 2, Figure 42).

3.7. Individual Tree Crown Delineation Methodology

During the literature review multiple approaches were found for performing ITC delineation. The forest type, the density and the level of heterogeneity, are parameters that can affect the performance of delineation and segmentation algorithms. This variation in performance can be observed by the differences in the results of previous studies (Brandtberg et al., 2003; Heurich, 2008; Persson et al., 2002). A LM filtering approach solely based on the DSM, could be problematic in the detection of the smaller trees. However, an accuracy of 61% was achieved in the study of Nurhayati (2015) in the ITC methodology she proposed, which is comparable with results from similar studies (Gebreslasie et al., 2011; Gougeon and Leckie, 2006; Wang et al., 2004; Wulder et al., 2004). Based on the promising results, and the availability of ArcGIS and eCognition tools developed by Nurhayati (2015), the same method was followed in this study in order to delineate individual tree crowns. Also, it is important to note that the results of Nurhayati were based on the same tropical forest in a neighboring study area (different plots), thus expected to perform similarly.

The DSM and the orthomosaic (0.043m) of the plot Th01 were used as input data for the ITC delineation. The workflow of the basic processes is depicted in Figure 25, and the Chapters 3.7.1 to 3.7.3 refer to these processes; the treetop detection, the crown boundaries detection, and finally the point cloud segmentation and assignment of field survey tree per point cloud segment.

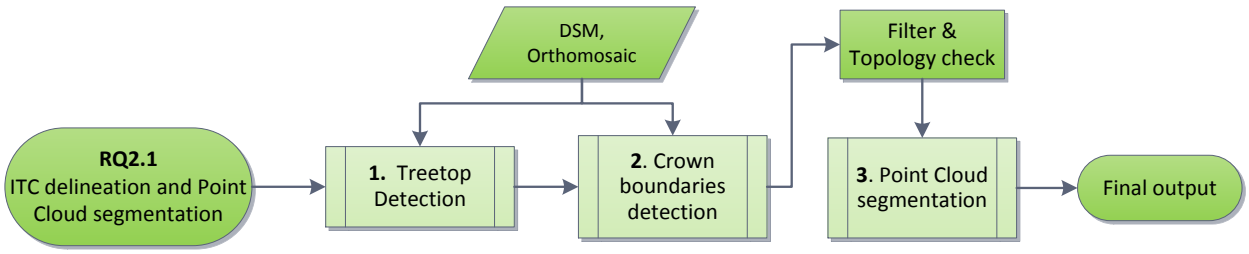

Figure 25. The GEOBIA approach for ITC delineation and individual tree point cloud segmentation.

3.7.1. Treetop Detection

In several studies the local maxima approach is based in CHM, reconstructed from LiDAR point clouds. For a minimization of false detections some studies refer to detection based on a canopy maxima model (CMM) (Chen et al., 2006; Monnet et al., 2010; Reitberger et al., 2009). In this case the treetop detection approach is based on finding peaks (LM), from variable window size on a smoothed DSM. The models in ArcGIS that were used, can perform the following steps, and for further documentation one can refer to Nurhayati (2015):

1. Initial DSM smoothing (focal statistics to derive mean, raster calculator for keeping high values)
2. DSM smoothing with varying degree of smoothness
3. Finding local maxima (focal statistics to derive maximum, raster to point)

4. Treetops estimation

It was necessary to include two more models, for retrieving plot boundaries on the DSM and orthomosaic (clip based on the point cloud boundaries, retrieved by lasboundaries - LAStools) and a final treetop selection (based on the A4 step of Nurhayati). The final treetops are exported as shapefile and will be used as seeds, for the detection of the crown boundaries in the next process.

3.7.2. Crown Boundaries Detection

A GEOBIA approach was followed for the crown boundaries detection, based on two rulesets in eCognition that can perform: a) a classification of shadow and gap areas and b) a detection of ITC. The chessboard segmentation and assignment of classes (based on tree height values), were used for the shadow and gaps classification. As input data the DSM and the orthomosaic was used. Next, a region growing method was used, taking advantage of the detected treetops of the previous step. Additional input layers for retrieving individual tree crown boundaries are produced by filtering the DSM values (Min/Max) and using Canny's Edge detection algorithm, for the region growing method. The rulesets in eCognition used for this purpose, were provided by Nurhayati (2015). The output of this operation is a shapefile containing all ITC as polygons.

Before the point cloud segmentation, it is essential to perform a filtering operation in the ITC polygons, in order to keep only complete (crowns near plot boundaries are split) and of significant size crowns (>0.44m^2). Also performing a topology check in ITC polygons can prevent errors before the point clouds segmentation.

The region growing approach for the ITC delineation as assessed by Nurhayati, is able to perform with an accuracy of 61% as on "perfect" detection of the crowns and around 18% of a "good" detection, overall an expected 79% ITC detection. The occurrences of splitting trees are estimated at 14%, while the false detection around 6%, attributed to errors of omission and commission.

3.7.3. Point Cloud Segmentation and Assignment of Field Survey Tree ID

Each tree should be represented by a PPC segment, in order to fit a geometric model and extract the TOC crown shape parameters. For the point cloud segmentation, the PolyClipData algorithm was used (FUSION software package) that can perform batch clipping based on ESRI shapefiles (Appendix 4).

Although the field survey data are georeferenced accurately based on the TLS trunks map in step RQ1.2, the final assignment of field tree id to each point cloud segment is still a process that needs visual interpretation. The proximity is the first rule of the assignment, meaning the closest field tree point from the segment has the higher chance of being the correct tree.

In case that multiple or none field tree points fall within one segment the DBH value and 3D visualization were taking into account for the correct assignment. RANSAC shape detector algorithm was used for deriving DBH in the TLS point cloud segments, and also for visualizing the trunk orientation, in Cloud Compare (Figure 26).

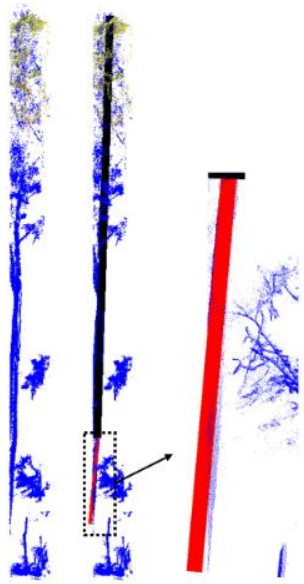

Figure 26. Example of the RANSAC algorithm in deriving DBH.

3.8. Model Fitting Approach for Extraction of Crown Shape Parameters

An overview of the processes towards answering the last research questions RQ 2.2 and RQ 3 is depicted in the flowchart in Figure 27. The Chapter 3.8.1 is addressing to RQ 2.2 where a hemi-ellipsoid crown modelling approach is proposed while Chapter 3.8.2 is addressing the RQ3, proposing a statistical analysis to show whether the parameters extracted by the hemi-ellipsoid approach are sufficient for species discrimination.

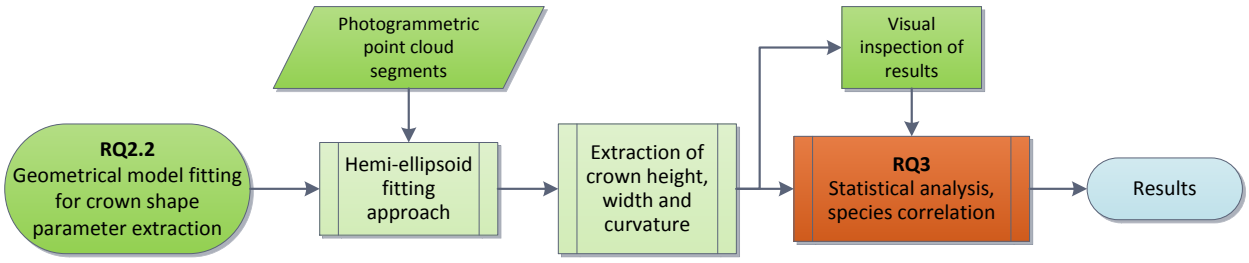

Figure 27. Flowchart of the methodology for RQ2.2 and RQ3.

3.8.1. Hemi-Ellipsoid Model

The data available for fitting, are the individual tree PPC segments that were retrieved based on the previous step. A geometric equation of a generalised hemi-ellipsoid was proposed by Sheng et al. (2001), for modelling coniferous tree crowns in order to optimize image-matching algorithms for individual tree delineation process from aerial orthophotos (Figure 28). This equation (Equation 2) is an adaptation of Pollock's (1996) three dimensional crown model, which is an extension of Horn's (1971) general model for the two-dimensional vertical profile of a crown envelops.

$$\frac{(Z + ch - Z_t)^{cc}}{ch^{cc}} + \frac{((X - X_t)^2 + (Y - Y_t)^2)^{cc/2}}{cr^{cc}} = 1 \quad (2)$$

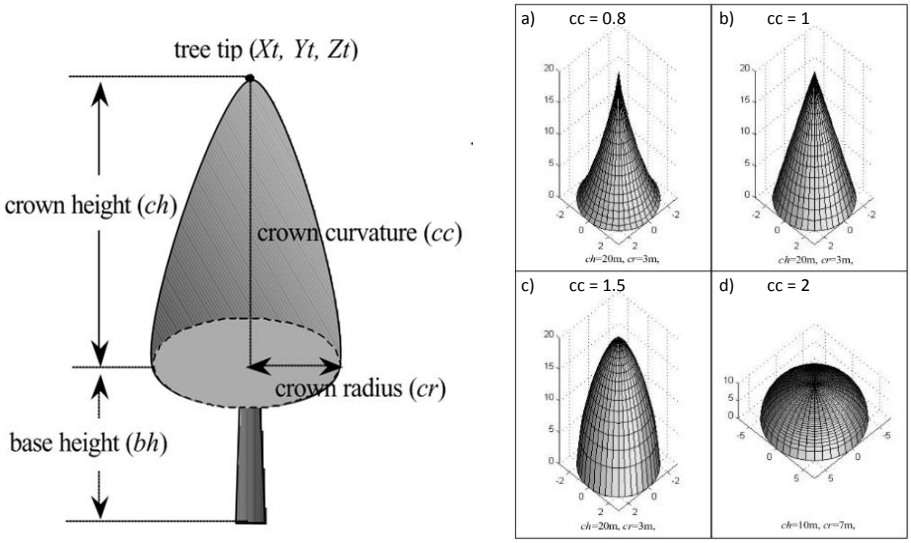

Figure 28. Parameters in the tree model and examples of different curvatures, as specified by Sheng et al. (2001).

The crown height (ch) and crown radius (cr) parameters correspond to the vertical and horizontal dimensions of a crown respectively. The upwards ($cc < 1$) or downwards ($cc > 1$) concavity of the crown is described by crown curvature (cc), with $cc = 1$ representing a straight line. Also the treetop coordinates correspond to (X_t, Y_t, Z_t) parameters.

In this case, the individual tree crowns are already delineated, based on the GEOBIA approach, so the geometric equation will be used for the extraction of the crown shape parameters (height, width and curvature). It is interesting to see whether there are patterns in these parameters in tropical forest trees, based on the Sheng's model and the TOC PPC segments.

The assistance of Dr. Juha Suomalainen made possible this modelling step. More specifically, in modifying appropriately the generalized ellipsoid (Equation 3) and aiding in scripting the iterative algorithm for the parameters extraction. The programming software that was used was MATLAB, the script can be found in Appendix 5.

The main processing of the script includes the scaling of the data for visualization purposes, the generation of the necessary input for the hemi-ellipsoid, the generation of a pixel grid for the top of canopy and the application of Equation 3. The extracted shape parameters include crown height, radius, curvature and the (X_t, Y_t, Z_t) treetop position within the specific point cloud based on finding LM within the point cloud.

The modified equation as used for the fitting process in Matlab:

$$((1-(x-X_t)^2+(y-Y_t)^2)^{\frac{\frac{cc}{2}}{|cr^{cc}|}\left(\frac{1}{cc}\right)*|ch|-|(ch+Z_t)|} + \left(\frac{0}{\left(cr>\sqrt{(x-X_t)^2+(y-Y_t)^2}\right)}\right) \quad (3)$$

Where the second part of the equation is there for producing NaN values outside of the ellipsoid. In total, 207 individual tree point clouds were tested with this modelling approach. Although, the model proposed by Sheng oversimplifies tree crowns in the real world, it was interesting to see whether this approach is adequate for extracting crown parameters and if they are consistent for other applications.

3.8.2. Hemi-Ellipsoid Fitting and Extracted Parameters Assessment

The assessment of the fit was done manually by visual inspection of the hemi-ellipsoid derived graphs for each segment, in order to decide if this method is sufficiently describing the crown surface and what are the possible reasons if not. The quality of the segmentation is expected to affect the performance of the ellipsoid fit.

For those trees of which the outcome of the modelling is considered as sufficient, their extracted shape parameters will be included in the statistical analysis to investigate whether there are patterns in these parameters for specific clusters of tree species. For the statistical analysis initially a box-and-whisker plot will be created, to show the variation within the parameters on the different dominant species. Furthermore, 3D plots will be created to visualize the data and identify possible clusters. The software package used for this statistical analysis is RStudio.

4.1. Treetop Detection, ITC Delineation and Point Cloud Segmentation

During the treetop detection process 261 treetops were detected. From the field survey, there are 226 tree records available (of DBH >10cm). The numbers are relatively comparable; an overestimation of treetops could be attributed to the misidentification of bigger branches as individual trees. This can be verified in Figure 29; multiple treetops were false detected in an area of a fallen tree, as identified by the orthomosaic. Overall, the performance of this approach, is comparable with the results Nurhayati achieved in her research.

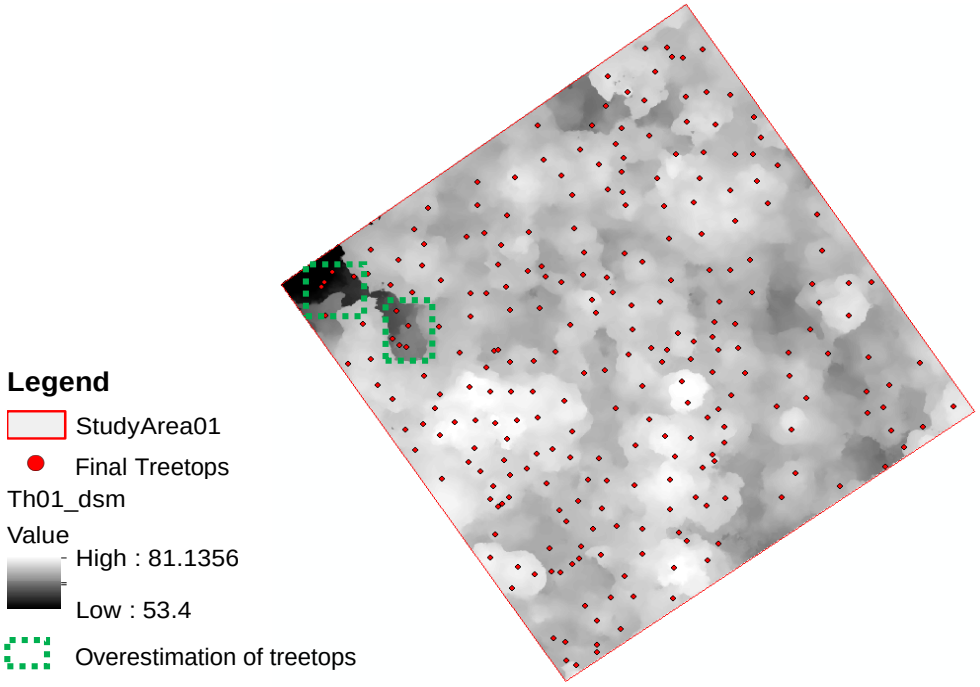

Figure 29. Final Treetops detected in the study area (Plot Th01).

Before the ITC delineation the shadow and gap areas were identified and excluded from the process. The crowns intersecting with the plot boundaries were removed, and smaller polygons were filtered out (Figure 43, Appendix 3), resulting in the most representative polygons. The 207 polygons that remained (Figure 30) were used for the PPC and the TLS point cloud segmentation (Figure 31). The PPC segments will be used for the modelling part while the TLS point cloud will be used for validation. Results showed an accuracy of 69,19% of good segmentation and of 30.81% of bad segmentation. An example of what is considered as a representative point cloud segment (good and bad), is depicted in Figure 32.

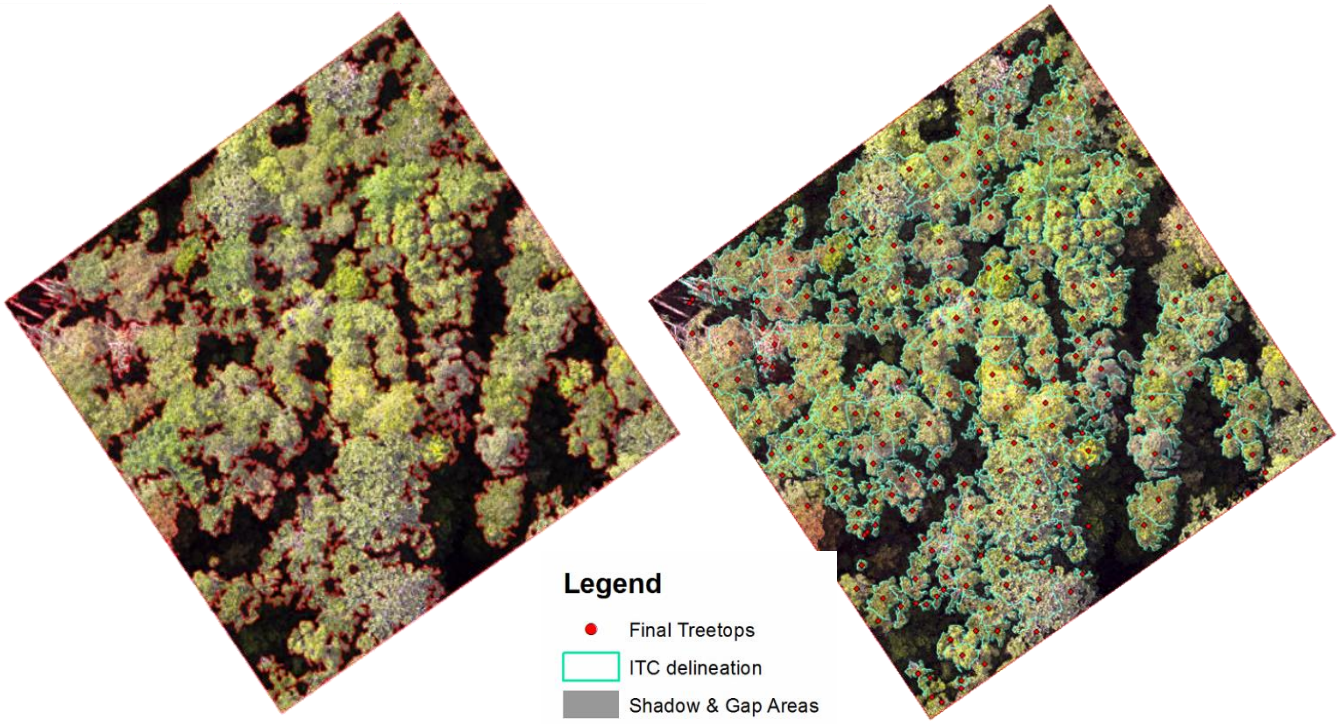

Figure 30. Left: The detection of shadow & gaps areas. Right: The result of the ITC delineation process in the orthomosaic with the final treetops.

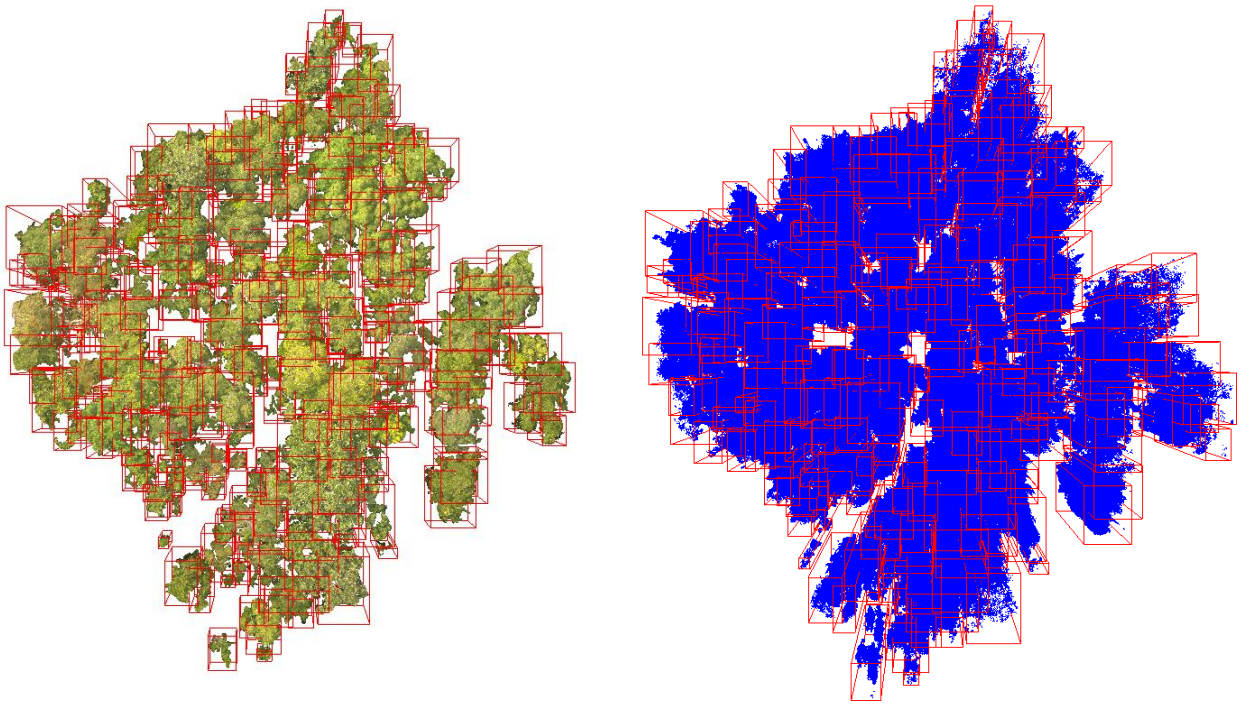

Figure 31. Left: Segmentation of RGB point clouds. Right. The TLS point cloud segments, in FUSION.

4.2. Inventory of Point Cloud Segments with Field Survey Measurements

Each of the 207 tree point cloud segments was linked with one field survey tree record based on proximity, DBH measurements and 3D visualization. A visual inspection confirmed that the correct survey ID was assigned to each segment. Results showed that if only proximity was considered there would be more than 30% mismatches due to the complexity of the study area. In some segments the trunk on breast height, was not visible or was located in the edges of the segment since trees do not grow completely vertical but spread in different directions due to ecological reasons, such as the competition for space (Figure 33). For further valid comparisons, regardless of the segmentation accuracy, each segment must be assigned with the accurate field tree. From the 207 segments of tree point clouds, 172 were successfully matched with a field survey tree record based on proximity, DBH and 3D visualization when applicable.

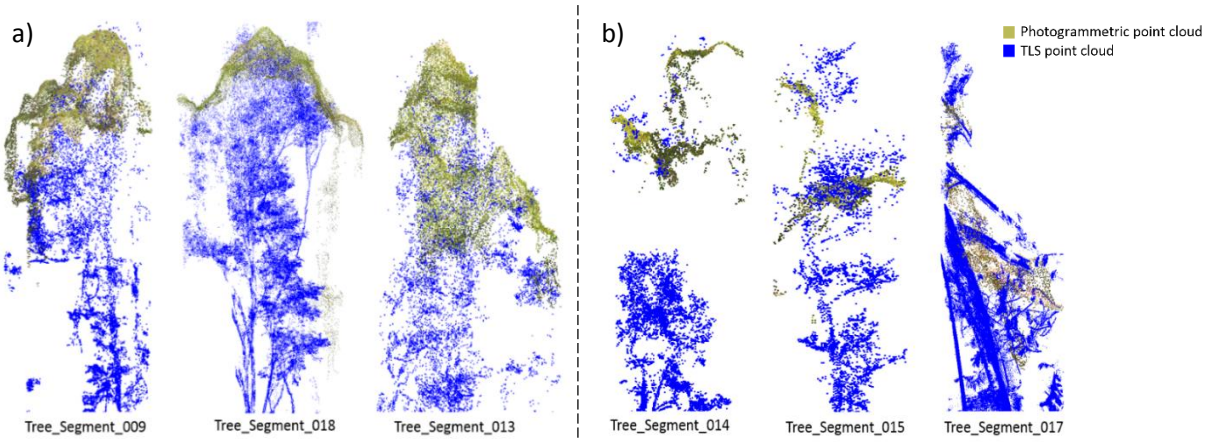

Figure 32. Example of individual tree point cloud segments, a) good segmentation b) bad segmentation.

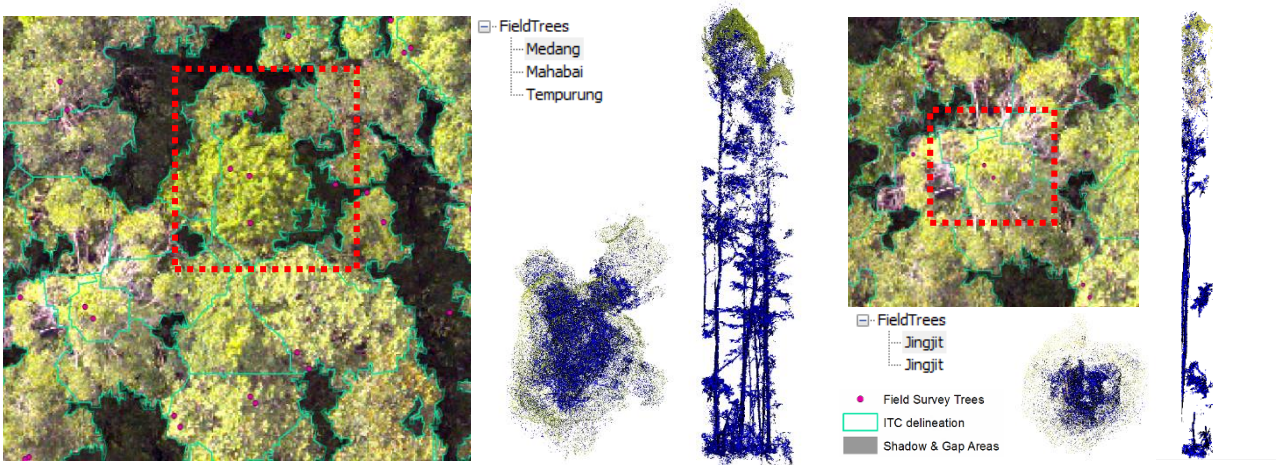

Figure 33. Left: Example of three field tree records falling in one segment. Right: An example of two field records falling in one segment while the trunk in breast height is in a different segment.

4.3. Modelling Approach based on the Hemi-Ellipsoid Fitting

For the 172 segments that could be linked to field information, the results of ellipsoid fit approach were classified as “adequate” or “non-adequate” based on visual interpretation (Figure 34). The extracted parameters from segments that were sufficiently described by the ellipsoid fit will be further used for the statistical analysis.

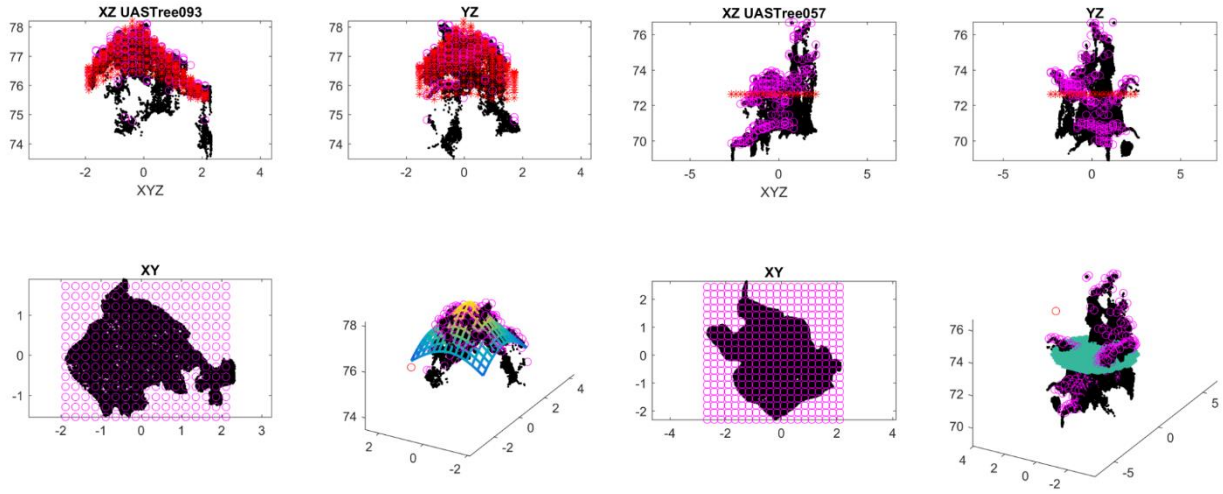

Figure 34. Left: Example of adequate fit of the ellipsoid. Right: Example of failure, due to bad segmentation.

The visual inspection showed that the model fitting approach resulted in a 54.07% success of adequate fit with 30.23% being characterized as very good fit. An example of different types of fitted trees can be find in Figure 35. The remaining 45.93% categorized as non-successful fit was further investigated in order to identify the possible reasons. Three basic reasons for the model failure were identified; (1) erroneous segmentation, (2) insufficient points in the point cloud, and (3) limitation of the model (oversimplified) or limitations of the input data (complexity).

The erroneous segmentation is attributing with 30.81% to the non-successful fit, and includes under- and over-segmentation. The under-segmentation; main tree canopy is partially outside of the segment and over-segmentation; multiple trees are within the same segments. Furthermore, a 3.49% of the non-successful fit is attributed to segments with insufficient amount of points for the fitting process, while a 15.12% had no apparent reason for the non-sufficient fit, thus attributed to the simplicity of the ellipsoid model compared to the complexity of dense forest canopy or the way PPC data are reconstructed. More specifically the model showed sensitivity (confusion) in segments of sparse points, and segments containing double (or more) peaked trees. With this approach the upper part of the tree’s crown was fitted to the hemi-ellipsoid model, since the PPC can only reconstruct the TOC. The hemi-ellipsoid model succeeded in extracting the shape parameters; (upper) crown height, width and crown curvature.

The shape parameters of 93 segments classified as “adequate” and can be further used for statistical analysis. Within these 93 segments 31 different species are present. Since for many species the samples were not enough for making valid assumptions only the species with at least four samples were tested. The shape parameters of eight different species were tested in the statistical analysis, which are presented in Table 3.

Table 3. Samples for statistical analysis.

Local Name	Number of samples
Jingjiit	9
Meranti	5
Nyatok_Babi	6
Pelawan	5
Perawas	5
Samak	11
Ubar	15
Terantang	5

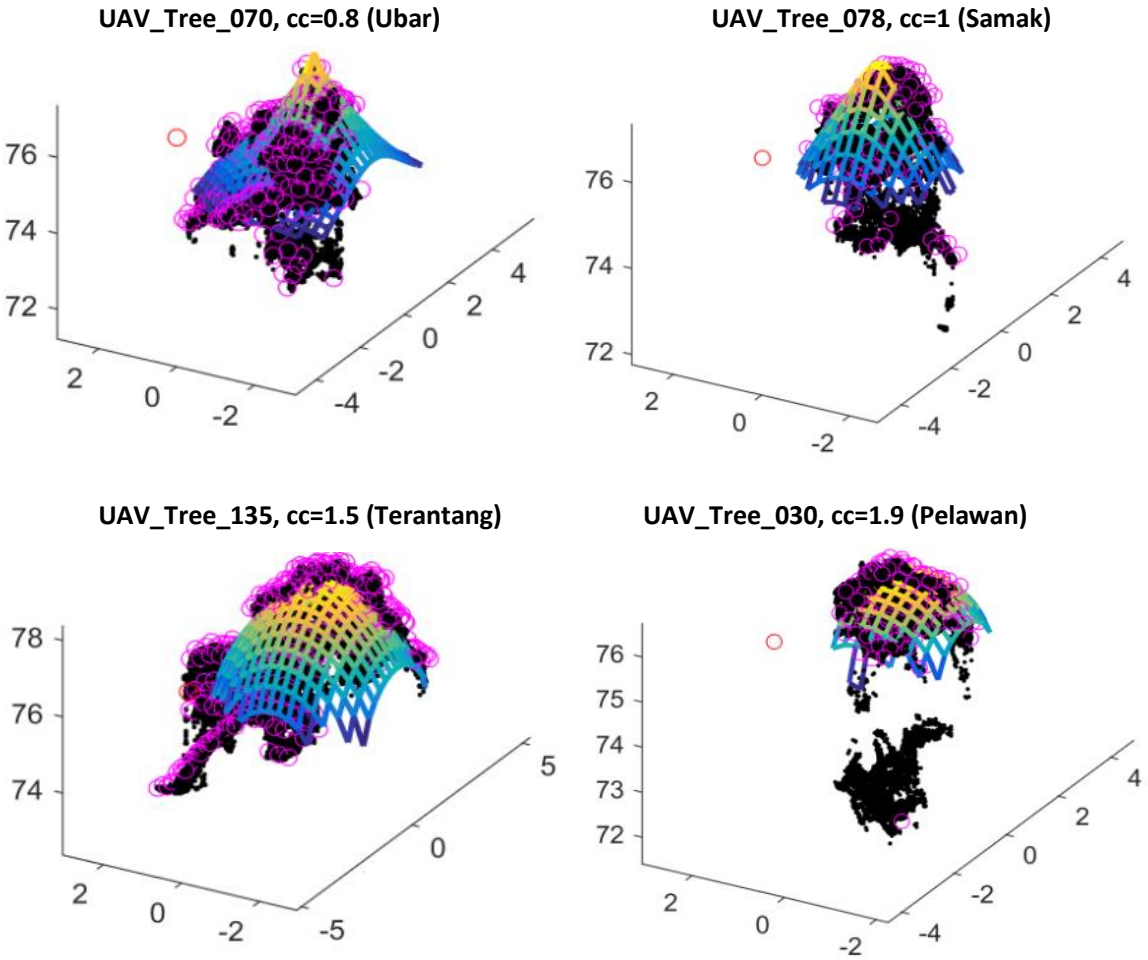

Figure 35. Different types of trees based on crown curvature, fit was classified as “very good”.

4.4. Statistical Assessment of the Parameters for Species Discrimination

Based on the eight different species that have enough samples, a box-and-whiskers plot initially was created to see the variation and skewness of the data, and how the parameters differ within species (Figure 36). From this plot we observe that some samples behave as outliers, while there is no significant variation between the different species. However, some trends were considered to be worth further investigation. Therefore, a 3D plot visualization was used to identify possible clusters.

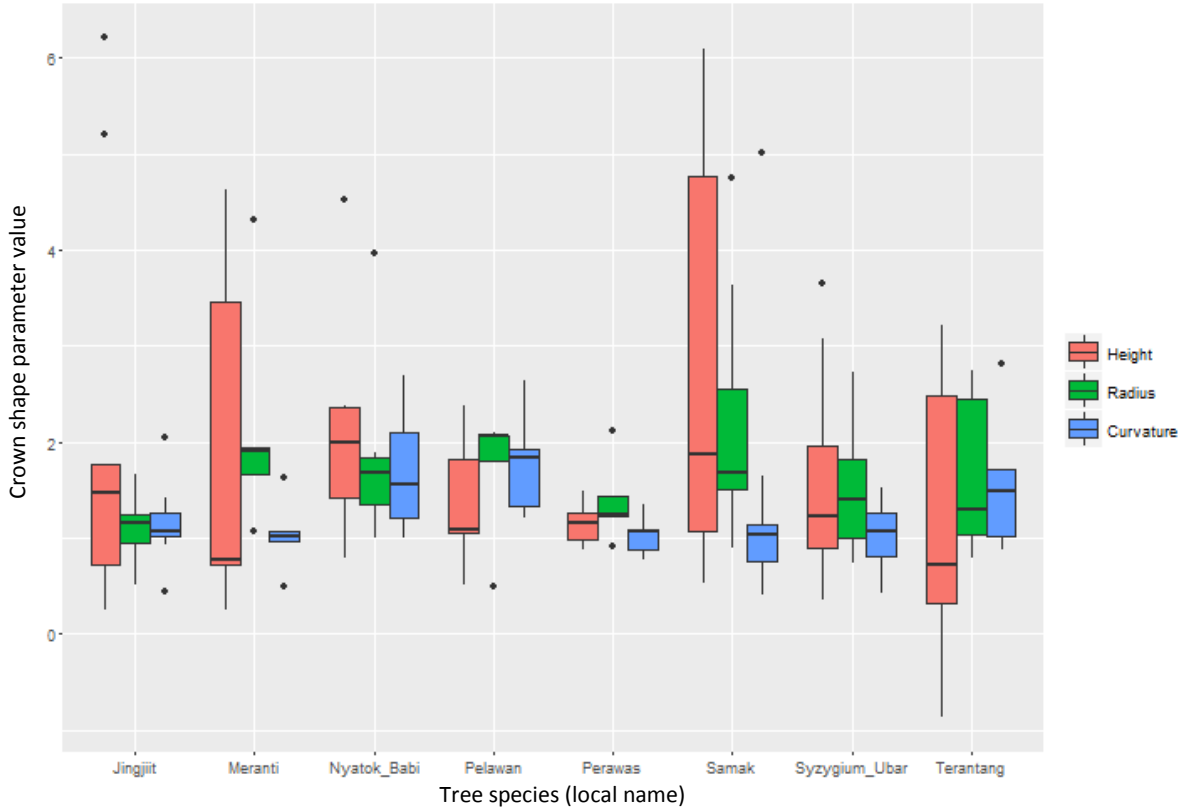

Figure 36. Box-and-whiskers plot of species and shape parameters variations.

Based on the trends that appear in the box-plot we can conclude the following:

- Relative upper crown height cannot be useful for species discrimination. However, it could be useful for other purposes as it can detect and parameterize trees that emerge either due to their height difference or due to their location conditions (near gaps or sparse canopy area) within the forest.
- Relative upper crown radius shows differentiation between some of the species (Jingjiit and Pelawan)
- Crown curvature shows differentiation between some of the species such as:
  Nyatok Babi, Pelawan and Terantang, which are expected to have a downward concavity compared to the other species.

The 3D plot in Figure 37, confirms that based exclusively on shape parameters it is not possible to delineate between all eight species because the differences between them are not significant enough. However, there are some species that can be separated from others:

- Perawas samples, show clustering effect when compared with Samak, Terantang, Pelawan and Jingjiit (Figure 38).
- Pelawan samples, show clustering effect when compared with Ubar and Jingjiit (Figure 39).

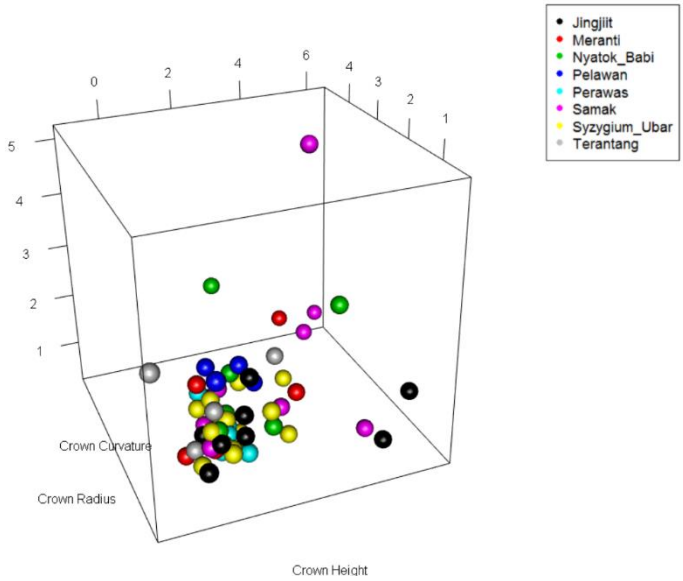

Figure 37. 3D scatterplot of species samples and their shape parameters.

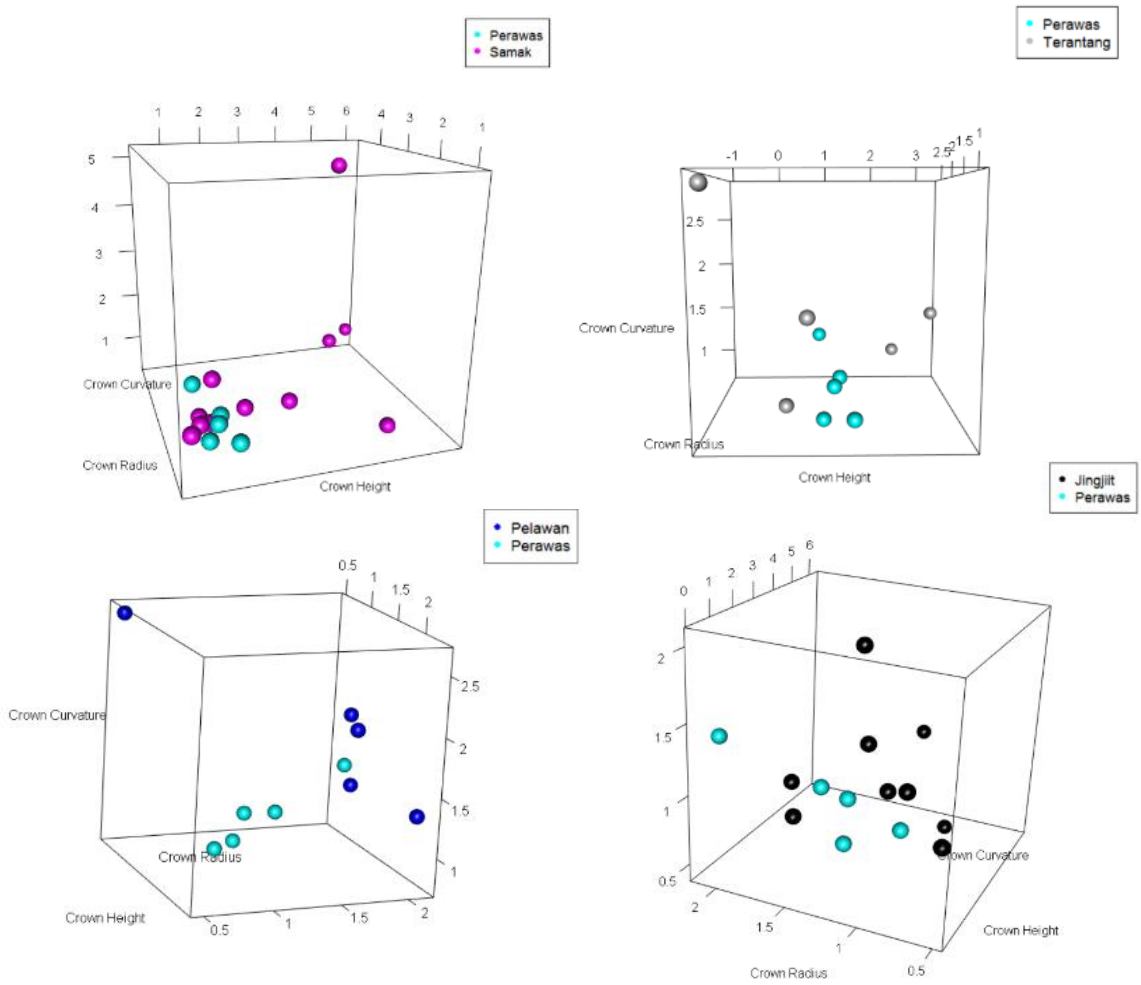

Figure 38. Example of clustering of Perawas in pairs comparison with other species.

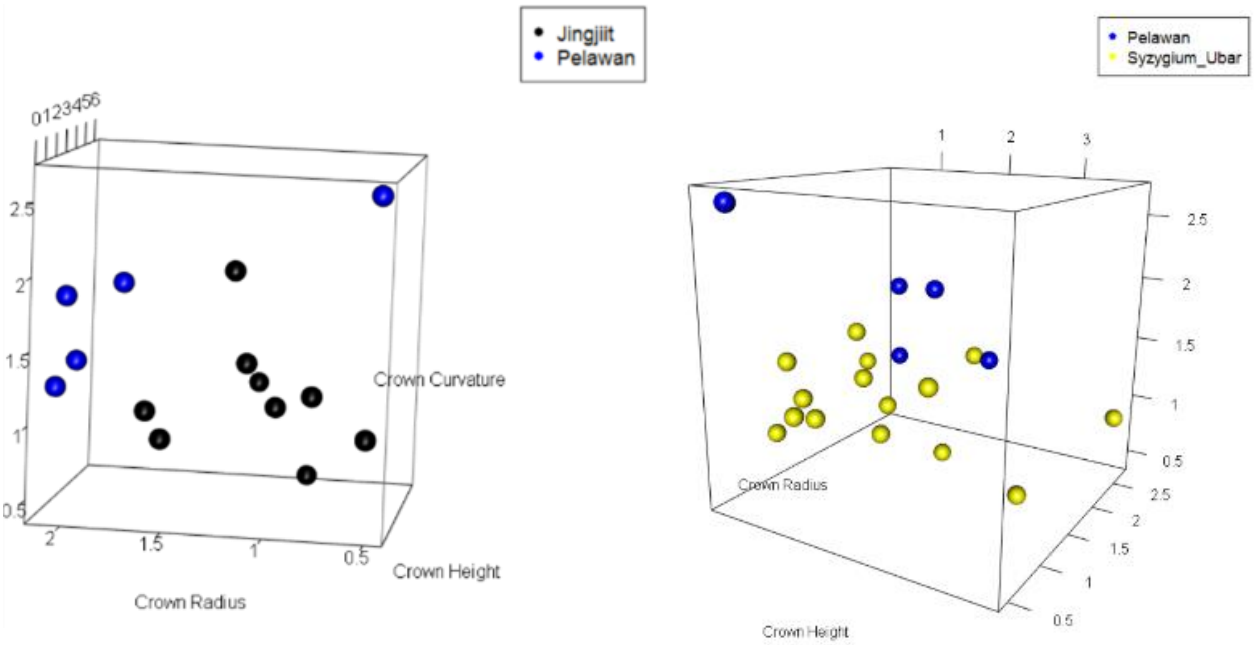

Figure 39. Example of clustering of Pelawas in pairs comparison with Jingjiit and Syzygium_Ubar.

An ecological investigation is needed to assess whether these parameters actually coincide with the real tree shape attributes which is out of the scope of this study but highly recommended for a future study.

5. Discussion

This chapter discusses the results derived from both the processing of the data and the statistical analysis. It is structured in a way to provide answers to the research questions. The first two sections discuss the technical parts of this study while the last part refers to the overall importance of crown shape parameters in forest inventories and to the limitations as identified from the statistical analysis.

5.1. Co-Registration of the Data

RQ1. Can a semi-automated methodology be applied for co-registration of UAV, TLS and field survey data?

The accurate co-registration of multi-source data always was and always will be the most important pre-processing step within the field of remote sensing while the selection of the appropriate method for the co-registration is an issue of attention. This is because it ensures that further processing will not be affected by spatial errors and valid comparisons or combinations can be made with the co-registered data. In dense tropical forests and also in the present study, it was expected that the co-registration of the TLS-based data with the UAV-based data is affected by the attenuation of the GPS signal on the TLS. Also, for the co-registration of the field data with the TLS-based data, it was evident that spatial transformations were needed in order to achieve the co-registration.

Within this study multiple software packages were tested in order to achieve the co-registration of multi-source data. The co-registration approach was not enabled by GCP's information, and the plot boundaries were not reliable; only after the first step of the co-registration where geo-referenced was applied. The aim of the co-registration step was to make available the boundaries of the study area, the TLS point cloud and field survey data in global coordinate system without geo-referencing errors.

The methodology for the co-registration between point clouds was based on previous studies that showed promising results on the use of the ICP algorithm. However, in the first part (RQ1.1) the ICP algorithm did not perform as good as expected. Different approaches were tested in order to identify why there are limitations in the use of ICP algorithm for an automated co-registration of forest canopy point clouds. For that reason, the TLS point cloud was also clipped to describe only the TOC as the RGB point cloud, to assess if this helps in optimizing the matching of the set of distance measurements. However, there was no improvement on the results of the ICP.

Although visually the point clouds appear similar, in terms of distance measurements they are not similar enough for the algorithm to overcome false detection of possible matches. The main drawback as it was identified, is due to the major structural differences of the two point clouds (density and spatial distribution of points). Maybe another approach would be to subsample the

TLS point cloud, and extract only the maximum height points mimicking the result of PPC, and then apply the ICP algorithm. Due to time limitation this was not investigated any further but improvements on the ICP algorithm such as the concept of deletion mask proposed by Marani et al. (2016) might increase the performance of the co-registration. The results of the rough alignment based on meshes deriving from the point clouds, were sufficient for the co-registration of the point clouds in this case.

The methodology proposed for the co-registration of TLS derived trunks map with the field survey tree locations was successful, and to my knowledge no similar approach was described before in literature. The ICP algorithm in this case worked sufficiently, and this permitted a high accuracy of co-registration between the field survey tree locations with the point cloud data.

5.2. Extraction of Crown Shape Parameters

RQ2. How the crown shape parameters can be extracted from the point clouds, and orthomosaics?

In order to derive the individual point cloud segments, a GEOBIA approach was followed for ITC delineation. The accuracy of the detection of treetops can be directly correlated with the overall accuracy of the ITC delineation, since the region growing approach is depending on the treetops as seeds.

The accuracy of the ITC delineation based on the segmentation results of this study is 69,19% which is comparable to 69.22% (Singh et al., 2015), 70% (Sium, 2015) and 61.39% (Nurhayati, 2015) for tropical forests. Previous studies show varying accuracies from 67% (Gougeon and Leckie, 2006) to 85% (Gebreslasie et al., 2011) in plantation forests, while higher accuracies can be achieved with ALS 96% (Kumar, 2012). The variations are depending on the resolution of the input data and the complexity of study area. For tropical forests when using VHR images and GEOBIA an accuracy of less than 70% is generally expected.

The hemi-ellipsoid fitting approach successfully modelled 54.07% of the trees, with 30.23% being characterized as with very good fit after visually inspection. To my knowledge there are no other studies deriving upper crown shape parameters from photogrammetric point clouds in tropical forests, in order to compare the model fitting approach results. Based on the achieved results, this method can extract the upper crown shape parameters: relative crown height and width, crown curvature, and tree peak location within the segment (Xt, Yt, Zt).

Since, this model is the simplest way to represent a complex shape, such a tropical forest tree crown derived by a photogrammetric point cloud, the results of the fit are considered as adequate. Besides the hemi-ellipsoid approach, during this research, first a full-ellipsoid approach was tested but the results were not adequate. The full-ellipsoid showed significantly less differentiation between the segments, mainly due to the way points are distributed within these segments (*i.e.* not following a bell crown shape) (Figure 40).

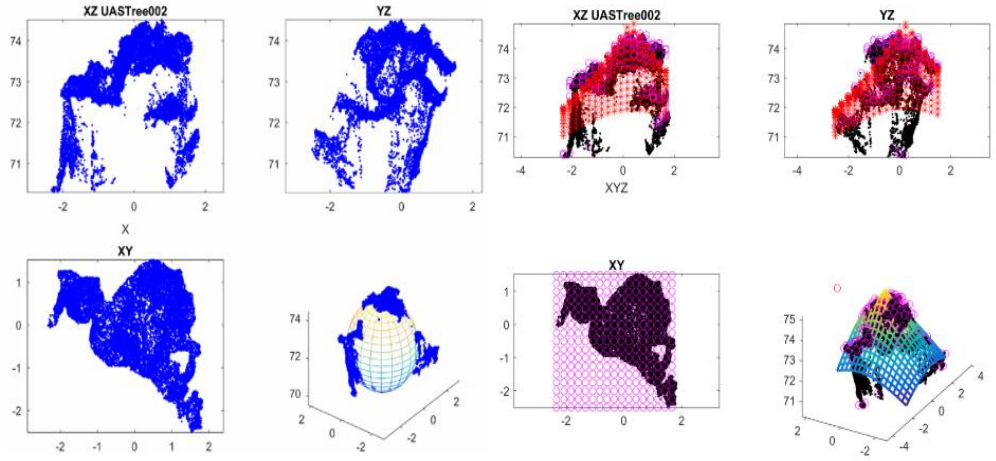

Figure 40. Example of the full-ellipsoid and hemi-ellipsoid approaches for parameter extraction.

Below the main reasons of failure for the hemi-ellipsoid modelling approach are listed as identified during the data processing and analysis, in order of bigger to smaller impact:

- ITC delineation and segmentation accuracy. The over- and under-segmentation plays a major role as the hemi-ellipsoid performance is limited when more than one tree crown is inside the segment or a tree crown is split. Perhaps a pre-processing step of filtering out the excessive peaks in the point cloud segments, would help in the cases of over-segmentation. In cases of under-segmentation, the specific segments that are split must be merged in order to be included to the modelling phase, however this would demand an advanced 'matching' step for the identification of these segments.

- The point clouds are reconstructed from a structure from motion process. The distribution of points and the density is not an exact representation of the real tree but an approximation. There is a level of uncertainty on how this approximation corresponds when looking at an individual tree level for advanced issues such as differences between tree species in a tropical forest.

- The hemi-ellipsoid model. A hemi-ellipsoid is a simplified way to represent a tree crown, as trees can be seen as 3D objects with horizontal and vertical dimensions, but no other information is taken into account. However, considering the uncertainty of the PPC approximation of trees representation it is justified to use a simplified model for the fitting approach.

5.3. Consistency and Usability of the Crown Shape Parameters

RQ 3. Are these parameters consistent and which are possible uses for these parameters?

In order to test the consistency of the shape parameters, a statistical analysis was performed in R, to show if there is any correlation between species and the extracted crown shape parameters. The box-and-whiskers plot showed that the variation between the parameters is not significant enough to differentiate between the eight different species but some species show separation from others. From the 3D plot containing all species, no apparent clustering was identified. However, in paired 3D comparison, Pelawan and Perawas samples clustering was observed, compared to some of the other species.

Crown curvature could be more useful in species discrimination compared to crown height and width, because the vertical and horizontal dimensions could be influenced by environmental parameters. There are many parameters that could result in shape differences even within the same species such as: tree's age, tree's health, location, environmental conditions, adaptation, competition for light and space etc. In order to minimize the influence of these parameters a larger amount of samples is necessary, and of course a priori knowledge of the trees actual shape differences.

While there are traits of differentiation between different species by observing the shape parameters, it would not be feasible to perform a species classification at this stage exclusively based on these parameters in tropical forests. However, a species identification based on these parameters could have better results in forests composed of fewer species. It is possible that in combination with spectral information, structural parameters could increase the classification accuracy as showed in the study of St-Onge et al. (2015). In order to assess the trends of shape parameters observed between these species, a background on forestry and on the specific tropical tree species is necessary. This exceeds the purposes of this study but could be addressed as a topic for future research.

Overall, the crown shape parameters are very important towards conservation measures. Detection of disturbances within the forest is feasible based on change detection techniques. The parameters are useful for modelling and management applications such as growth monitoring, forest fire or disease distribution simulations, and thinning operations. A detailed forest inventory containing species distribution, shape parameters, treetop location and other parameters would allow management policies to monitor exploitation activities more efficiently within region or national inventories and for programs such as REDD+.

6. Conclusions

The main objective of this research was to extract tree crown shape parameters from the photogrammetric point cloud. For this purpose, a methodology was proposed for the co-registration of multi-source data, ITC delineation and point cloud segmentation, and a geometric model fitting. A secondary objective was to assess the consistency of the crown shape parameters. The following three paragraphs correspond to the three research questions and present the conclusions drawn based on the results.

The semi-automated approach demonstrated that the co-registration of multi-source data is possible without the use of field GCP's. The point cloud data were co-registered based on a transformation matrix retrieved from a rough alignment of the generated meshes. The ICP algorithm showed limitation on the fine alignment of PPC and TLS point cloud. On the other hand, the ICP algorithm increased the co-registration accuracy of the field data with the TLS point cloud. Differences in point density and spatial distribution of the points within the PPC and TLS point cloud, interfere with the performance of the ICP algorithm.

Taking advantage of the already well implemented GEOBIA approach available by Nurhayati, the ITC delineation achieved an 69.19% accuracy, comparable with previous studies. The hemi-ellipsoid geometric model fitting approach that was proposed succeeded in fitting 54.1% of the segments, allowing further statistical analysis. Bad segmentation is identified as the main reason of fitting failure, while the tree crown approximation based on the PPC in combination with the simplified hemi-ellipsoid approach affect also the fitting success.

The statistical analysis showed that species discrimination based exclusively on crown shape parameters deriving from airborne photogrammetric point clouds, is not possible for all species within the tropical forest. Trees of the species Perawas and Pelawan showed clustering and could be separated by some of the other species in paired comparison.

The crown height, width and curvature are parameters that could be of use in various simulation applications for forest management such as for growth monitoring, thinning, pruning, clearing, prescribed burning, forest fire and disease spread modelling. Crown curvature is more appropriate for species discrimination than crown height and radius, but further investigation is needed.

7. Recommendations

This chapter consists of recommendations for future studies. Problems and potential solutions are presented, as identified during the data pre-processing, processing and analysis phases.

Automation of the co-registration of multi-source data

There are two ways towards automation of co-registration of the PPC and TLS point cloud (RQ1.1). Either with optimizing the meshes alignment or direct alignment of the point clouds. When the alignment is based on meshes, an advanced image matching algorithm is needed in order to automate the rough alignment process, instead of manually selecting sphere pairs. For the direct alignment of point clouds, further investigation is needed on how to overcome the structural differences of points clouds, deriving from different sources, that affect the matching algorithms as shown in the ICP algorithm.

In step RQ1.2 the trunks location map was created by manually picking the points of visually identified trunks. Another approach that was partially tested is the use of RANSAC algorithm in automating the trunks detection as cylindrical objects. The initial tests showed false cylinder detections by RANSAC, attributed to high sensitivity to noise. Noise can be partially filtered out by setting threshold values for minimum and maximum circumference, in cylinder detection of the RANSAC algorithm which is worth of further investigation.

Accuracy of the ITC delineation and the model fitting approach

An increase in the ITC delineation accuracy could lead to better fit results in the hemi-ellipsoid model. When it is applicable, the use of ALS or TLS point cloud data as input for the GEOBIA approach might result to higher ITC delineation accuracy. Further investigation is needed on the way reconstructed photogrammetric point clouds from VHR images represent real objects as trees.

Background knowledge regarding the tropical tree species

In order to investigate further the crown shape parameters consistency and their correspondence to species, forestry background is necessary. It is recommended that field experts regarding tropical tree species can confirm if the derived crown curvature by the extracted parameters coincides with the actual species crown curvature.

References

Alonzo, M., Bookhagen, B., Roberts, D.A., 2014. Urban tree species mapping using hyperspectral and lidar data fusion. Remote Sensing of Environment 148, 70–83. doi:10.1016/j.rse.2014.03.018

Andrews, P.L., 2009. BehavePlus fire modeling system, version 5.0: Variables General Te, 111.

Armenakis, C., Gao, Y., Sohn, G., 2013. Co-registration of aerial photogrammetric and LiDAR point clouds in urban environments using automatic plane correspondence 155–166. doi:10.1007/s12518-013-0105-9

Beauchemin, M., Thomson, K.P.B., Edwards, G., 1998. On the Hausdorff distance used for the evaluation of segmentation results. Canadian Journal of Remote Sensing 24:1, 3–8. doi:10.1080/07038992.1998.10874685

Besl, P.J., McKay, H.D., 1992. A Method for Registration of 3-D Shapes.

Blaschke, T., 2010. Object based image analysis for remote sensing. 5ISPRS6 Journal of Photogrammetry and Remote Sensing 65, 2–16. doi:10.1016/j.isprsjprs.2009.06.004

Blaschke, T., Hay, G.J., Kelly, M., Lang, S., Hofmann, P., Addink, E., Queiroz Feitosa, R., van der Meer, F., van der Werff, H., van Coillie, F., Tiede, D., 2014. Geographic Object-Based Image Analysis - Towards a new paradigm. ISPRS Journal of Photogrammetry and Remote Sensing 87, 180–191. doi:10.1016/j.isprsjprs.2013.09.014

Brandtberg, T., Walter, F., 1998. Automated delineation of individual tree crowns in high spatial resolution aerial images by multiple-scale analysis. Machine Vision and Applications 11, 64–73. doi:10.1007/s001380050091

Brandtberg, T., Warner, T. a., Landenberger, R.E., McGraw, J.B., 2003. Detection and analysis of individual leaf-off tree crowns in small footprint, high sampling density lidar data from the eastern deciduous forest in North America. Remote Sensing of Environment 85, 290–303. doi:10.1016/S0034-4257(03)00008-7

Burt, A., Disney, M.I., Raumonen, P ., Armston, J., Calders, K., Lewis, P., 2013. Rapid characterisation of forest structure from TLS and 3D modelling. Igarss 3387–3390.

Buss, S.R., 2003. 3-D Computer Graphics, A Mathematical Introduction with OpenGL, Cambridge University Press.

Calders, K., Newnham, G., Burt, A., Murphy, S., Raumonen, P., Herold, M., Culvenor, D., Avitabile, V., Disney, M., Armston, J., Kaasalainen, M., 2015. Nondestructive estimates of above-ground biomass using terrestrial laser scanning. Methods in Ecology and Evolution 6, 198–208. doi:10.1111/2041-210X.12301

Chen, Q., Baldocchi, D., Gong, P., Kelly, M., 2006. Isolating individual trees in a savanna woodland using small footprint lidar data. Photogrammetric Engineering & Remote Sensing 72, 923–932. doi:10.14358/PERS.72.8.923

Chen, Q., Qi, C., 2013. LiDAR Remote Sensing of Vegetation Biomass. Remote Sensing of Natural Resources 399–420. doi:doi:10.1201/b15159-28

Colomina, I., Blázquez, M., Molina, P., Parés, M.E., Wis, M., 2008. Towards a new paradigm for High-Resolution low-cost photogrammetry and Remote Sensing. XXIst ISPRS Congress: Technical Commission I XXXVII Par, 1201.

Couclelis, H., 2000. Modeling frameworks, paradigms, and approaches. Geographic Information Systems and Environmental Modelling 1–15.

Dalponte, M., Bruzzone, L., Gianelle, D., 2012. Tree species classification in the Southern Alps based on the fusion of very high geometrical resolution multispectral/hyperspectral images and LiDAR data. Remote Sensing of Environment 123, 258–270. doi:10.1016/j.rse.2012.03.013

Dorigo, W., Hollaus, M., Wagner, W., Schadauer, K., 2010. An application-oriented automated approach for co-registration of forest inventory and airborne laser scanning data. International Journal of Remote Sensing 31, 1133–1153. doi:10.1080/01431160903380581

Fagan, M., Defries, R., 2009. Measurement and Monitoring of the World ' s Forests. Resources for the Future 129.

FAO, 2014. State of the World's Forests, Food and Agriculture orginization of the United Nations.

FAO, 2010. FRA 2010 – Country Report, Indonesia. FAO Forestry Paper 163 340.

Fritz, a., Kattenborn, T., Koch, B., 2013. UAV-Based Photogrammetric Point Clouds – Tree Stem Mapping in Open Stands in Comparison to Terrestrial Laser Scanner Point Clouds. ISPRS - International Archives of the Photogrammetry, Remote Sensing and Spatial Information Sciences XL-1/W2, 141–146. doi:10.5194/isprsarchives-XL-1-W2-141-2013

Gebreslasie, M.T., Ahmed, F.B., van Aardt, J.A.N., Blakeway, F., 2011. Individual tree detection based on variable and fixed window size local maxima filtering applied to IKONOS imagery for even-aged Eucalyptus plantation forests. International Journal of Remote Sensing 32, 4141–4154. doi:10.1080/01431161003777205

Gorte, B., Pfeifer, N., 2004. Structuring laser-scanned trees using 3D mathematical morphology. International Archives of Photogrammetry and Remote Sensing 35, 929–933. doi:10.1.1.1.7844

Gougeon, F. a, Leckie, D.G., 2006. The individual tree crown approach applied to Ikonos images of a coniferous plantation area. Photogrammetric Engineering and Remote Sensing 72, 1287–1297. doi:10.14358/PERS.72.11.1287

Grainger, A., 2008. Difficulties in tracking the long-term global trend in tropical forest area. Proceedings of the National Academy of Sciences of the United States of America 105, 818–823. doi:10.1073/pnas.0703015105

Hansen, M.C., Stehman, S. V, Potapov, P. V, Arunarwati, B., Stolle, F., Pittman, K., 2009. Quantifying changes in the rates of forest clearing in Indonesia from 1990 to 2005 using remotely sensed data sets. Environmental Research Letters 4, 34001. doi:10.1088/1748-9326/4/3/034001

Hauglin, M., Lien, V., Næsset, E., Gobakken, T., 2014. Geo-referencing forest field plots by co-registration of terrestrial and airborne laser scanning data. International Journal of Remote Sensing 35, 3135–3149. doi:10.1080/01431161.2014.903440

Herold, M., Schiller, F., 2009. An assessment of national forest monitoring capabilities in tropical non-Annex I countries : Recommendations for capacity building Prepared by. Africa 22, 1–62.

Heurich, M., 2008. Automatic recognition and measurement of single trees based on data from airborne laser scanning over the richly structured natural forests of the Bavarian Forest National Park. Forest Ecology and Management 255, 2416–2433. doi:10.1016/j.foreco.2008.01.022

Holmgren, J., Persson, Å., 2004. Identifying species of individual trees using airborne laser scanner. Remote Sensing of Environment 90, 415–423. doi:10.1016/S0034-4257(03)00140-8

Holmgren, J., Persson, Å., Söderman, U., 2008. Species identification of individual trees by combining high resolution LiDAR data with multi-spectral images. International Journal of Remote Sensing 29, 1537–1552. doi:10.1080/01431160701736471

Holopainen, M., Vastaranta, M., Liang, X., Hyyppä, J., Jaakkola, A., Kankare, V., 2013. Estimation of Forest Stock and Yield Using LiDAR Data. Remote Sensing of Natural Resources 259–290. doi:doi:10.1201/b15159-20

Horn, H.S., 1971. The Adaptive Geometry of Trees. Princeton University Press, Princeton, 144pp.

Huang, J., You, S., 2012. Point cloud matching based on 3D self-similarity. Computer Vision and Pattern Recognition Workshops (CVPRW), 2012 IEEE Computer Society Conference on 41–48. doi:10.1109/CVPRW.2012.6238913

Hyyppa, J., Hyyppa, H., Litkey, P., Yu, X., Haggren, H., Rönnholm, P., Pyysalo, U., Pitkänen, J., Maltamo, M., 2000. Algorithms and Methods of Airborne Laser Scanning for Forest Measurements. International Archives of Photogrammetry, Remote Sensing and Spatial Information Sciences 36, 82–89. doi:10.1.1.150.8427

Jakubowski, M.K., Li, W., Guo, Q., Kelly, M., 2013. Delineating individual trees from lidar data: A comparison of vector- and raster-based segmentation approaches. Remote Sensing 5, 4163–4186. doi:10.3390/rs5094163

Kaartinen, H., Hyypp??, J., Vastaranta, M., Kukko, A., Jaakkola, A., Yu, X., Py??r??l??, J., Liang, X., Liu, J., Wang, Y., Kaijaluoto, R., Melkas, T., Holopainen, M., Hyypp??, H., 2015. Accuracy of kinematic positioning using global satellite navigation systems under forest canopies. Forests 6, 3218–3236. doi:10.3390/f6093218

Kato, A., Moskal, L.M., Schiess, P., Swanson, M.E., Calhoun, D., Stuetzle, W., 2009. Capturing tree crown formation through implicit surface reconstruction using airborne lidar data. Remote Sensing of Environment 113, 1148–1162. doi:10.1016/j.rse.2009.02.010

Kato, A., Schreuder, G.F., Calhoun, D., Schiess, P., Stuetzle, W., 2007. Digital Surface Model of Tree Canopy Structure From Lidar Data Through Implicit Surface Reconstruction. ASPRS Annual Conference, Tampa Florida, May 7-11.

Keane, R.E., Gray, K., Bacciu, V., Leirfallom, S., 2012. Spatial scaling of wildland fuels for six forest and rangeland ecosystems of the northern Rocky Mountains, USA. Landscape Ecology 27, 1213–1234. doi:10.1007/s10980-012-9773-9

Koch, B., 2013. Remote Sensing supporting national forest inventories NFA. FAO knowledge reference for national forest assessments 1–18.

Korpela, I., Dahlin, B., Schäfer, H., Bruun, E., Haapaniemi, F., Honkasalo, J., Ilvesniemi, S., Kuutti, V., Linkosalmi, M., Mustonen, J., Salo, M., Suomi, O., Virtanen, H., 2007. Single-tree forest inventory using LiDAR and aerial images for 3D treetop positioning, species recognition, height and crown width estimation. Iaprs Volume XXX, 227–233.

Kumar N., 2006. Multispectral Image Analysis Using the Object-Oriented Paradigm, CRC Press

Kumar, V., 2012. Forest Inventory Parameters and Carbon Mapping from Airborne LiDAR.

Latifi, H., Fassnacht, F.E., Müller, J., Tharani, A., Dech, S., Heurich, M., 2015. Forest inventories by LiDAR data: A comparison of single tree segmentation and metric-based methods for inventories of a heterogeneous temperate forest. International Journal of Applied Earth Observation and Geoinformation 42, 162–174. doi:10.1016/j.jag.2015.06.008

Ligtenberg, A., 2016. Spatial Modelling and Statistics (GRS-30306) Summary of the Theory.

Marani, R., Renò, V., Nitti, M., D'Orazio, T., Stella, E., 2016. A Modified Iterative Closest Point Algorithm for 3D Point Cloud Registration. Computer-Aided Civil and Infrastructure Engineering 31, 515–534. doi:10.1111/mice.12184

McGaughey, R.J., 2015. FUSION/LDV: Software for LIDAR Data Analysis and Visualization 182.

McRoberts, R.E., Tomppo, E.O., 2007. Remote sensing support for national forest inventories. Remote Sensing of Environment 110, 412–419. doi:10.1016/j.rse.2006.09.034

Moffiet, T., Mengersen, K., Witte, C., King, R., Denham, R., 2005. Airborne laser scanning: Exploratory data analysis indicates potential variables for classification of individual trees or forest stands according to species. ISPRS Journal of Photogrammetry and Remote Sensing 59, 289–309. doi:10.1016/j.isprsjprs.2005.05.002

Monnet, J.-M., 2013. Evaluation of a semi-automated approach for the co-registration of forest inventory plots and airborne laser scanning data. The conference of the research community on Lidar and Forest Ecosystems (SilviLaser) 1–8.

Monnet, J.-M., Mermin, É., 2014. Cross-Correlation of Diameter Measures for the Co-Registration of Forest Inventory Plots with Airborne Laser Scanning Data. Forests 2307–2326. doi:10.3390/f5092307

Monnet, J., Mermin, E., Chanussot, J., 2010. Tree top detection using local maxima filtering : a parameter sensitivity analysis.

Morsdorf, F., Meier, E., Kötz, B., Itten, K.I., Dobbertin, M., Allgöwer, B., 2004. LIDAR-based geometric reconstruction of boreal type forest stands at single tree level for forest and wildland fire management. Remote Sensing of Environment 92, 353–362. doi:10.1016/j.rse.2004.05.013

Nurhayati, R., 2015. Individual tree crown delineation in tropical forest using Object-based analysis of othoimage and digital surface model. Thesis Report GIRS-2015-35, Laboratory of Geo-Information Science and Remote Sensing 3–6.

Olofsson, K., Lindberg, E., Holmgren, J., 2008. A method for linking field-surveyed and aerial-detected single trees using cross correlation of position images and the optimization of weighted tree list graphs. SilviLaser 2008 95–104.

Ørka, H., Dalponte, M., 2013. Characterizing forest species composition using multiple remote sensing data sources and inventory approaches. Scandinavian Journal of Forest Research 28, 677–688. doi:10.1080/02827581.2013.793386

Orka, H.O., Gobakken, T., Naesset, E., Ene, L., Lien, V., 2012. Simultaneously acquired airborne laser scanning and multispectral imagery for individual tree species identification. Canadian Journal of Remote Sensing 38, 125–138. doi:10.5589/m12-021

Pascual, C., Martín-Fernández, S., García-Montero, L.G., García-Abril, A., 2013. Algorithm for improving the co-registration of LiDAR-derived digital canopy height models and field data. Agroforestry Systems 87, 967–975. doi:10.1007/s10457-013-9612-2

Persson, Å., Holmgren, J., Söderman, U., 2002. Detecting and measuring individual trees using an airborne laser scanner. Photogrammetric Engineering & Remote Sensing 68, 925–932.

Pimont, F., Parsons, R., Rigolot, E., de Coligny, F., Dupuy, J.L., Dreyfus, P., Linn, R.R., 2016. Modeling fuels and fire effects in 3D: Model description and applications. Environmental Modelling and Software 80, 225–244. doi:10.1016/j.envsoft.2016.03.003

Pollock, J., 1996. The Automatic Recognition of Individual trees in Aerial Images of Forests based on a Synthetic Tree Crown Image Model. Department of Computer Science, The University of British Columbia Date.

Popescu, S.C., Wynne, R.H., 2004. Seeing the trees in the forest: using lidar and multispectral data fusion with local filtering and variable window size for estimating tree height. Photogrammetric Engineering & Remote … 70, 589–604.

Pratihast, A.K., 2010. 3D tree modelling using mobile laser scanning data. International Institute for Geo-information Science and Earth Observation.

Pyysalo, U., Hyyppä, H., 2002. Reconstructing tree crowns from laser scanner data for feature extraction. IAPRS, vol XXXIV, Part 3B.

R Core Team (2015). R: A language and environment for statistical computing. R Foundation for Statistical Computing, Vienna, Austria. URL https://www.R-project.org/.

Raumonen, P., Kaasalainen, M., Åkerblom, M., Kaasalainen, S., Kaartinen, H., Vastaranta, M., Holopainen, M., Disney, M., Lewis, P., 2013. Fast Automatic Precision Tree Models from Terrestrial Laser Scanner Data. Remote Sensing 5, 491–520. doi:10.3390/rs5020491

Reinhardt, E.D., Scott, J.H., Gray, K., Keane, R.E., 2006. Estimating canopy fuel characteristics in five conifer stands in the western United States using tree and stand measurements. Canadian Journal of Forest Research 36, 2803–2814. doi:10.1139/x06-157

Reitberger, J., Krzystek, P., Stilla, U., 2008. Analysis of full waveform LIDAR data for the classification of deciduous and coniferous trees. International Journal of Remote Sensing 29, 1407–1431. doi:10.1080/01431160701736448

Reitberger, J., Schnörr, C., Krzystek, P., Stilla, U., 2009. 3D segmentation of single trees exploiting full waveform LIDAR data. ISPRS Journal of Photogrammetry and Remote Sensing 64, 561–574. doi:10.1016/j.isprsjprs.2009.04.002

Report of Central Kalimantan and GGGI, 2015. Central Kalimantan, Moving Towards Green Growth.

Riegl Laser Measurement Systems, 2014. RIEGL VZ-400. http://www.riegl.com/uploads/tx_pxpriegldownloads/10_DataSheet_VZ-400_2014-09-19.pdf 3–6.

Rosca, L.S., 2015. Reconstruction of Tropical Forest Top of Canopy using Airborne Structure from Motion and Terrestrial LiDAR Technologies.

Shahzad, M., Schmitt, M., Zhu, X.X., 2015. Segmentation and Crown Parameter Extraction of Individual Trees in an Airborne Tomosar Point Cloud. ISPRS - International Archives of the Photogrammetry, Remote Sensing and Spatial Information Sciences XL-3/W2, 205–209. doi:10.5194/isprsarchives-XL-3-W2-205-2015

Sheng, Y., Gong, P., Biging, G.S., 2001. Model-based conifer-crown surface reconstruction from high-resolution aerial images. Photogrammetric Engineering and Remote Sensing 67, 957–965.

Singh, M., Evans, D., Tan, B.S., Nin, C.S., 2015. Mapping and Characterizing Selected Canopy Tree Species at the Angkor World Heritage Site in Cambodia Using Aerial Data. Plos One 10, e0121558. doi:10.1371/journal.pone.0121558

Sium, M.T., 2015. Application of Very High Resolution Imagery and Terrestrial Laser Scanning for Estimating Carbon Stock in Tropical Rain Forest of Royal High Resolution Imagery and Terrestrial Laser Scanning for Estimating Carbon Stock in Tropical Rain Forest of Royal Bel.

Sodhi, N.S., Posa, M.R.C., Lee, T.M., Bickford, D., Koh, L.P., Brook, B.W., 2010. The state and conservation of Southeast Asian biodiversity. Biodiversity and Conservation 19, 317–328. doi:10.1007/s10531-009-9607-5

St-Onge, B., Audet, F.-A., Bégin, J., 2015. Characterizing the Height Structure and Composition of a Boreal Forest Using an Individual Tree Crown Approach Applied to Photogrammetric Point Clouds. Forests 6, 3899–3922. doi:10.3390/f6113899

Suomalainen, J., Anders, N., Iqbal, S., Roerink, G., Franke, J., Wenting, P., Hünniger, D., Bartholomeus, H., Becker, R., Kooistra, L., 2014. A Lightweight Hyperspectral Mapping System and Photogrammetric Processing Chain for Unmanned Aerial Vehicles. Remote Sensing 11013–11030. doi:10.3390/rs60x000x

Suratno, A., Seielstad, C., Queen, L., 2009. Tree species identification in mixed coniferous forest using airborne laser scanning. ISPRS Journal of Photogrammetry and Remote Sensing 64, 683–693. doi:10.1016/j.isprsjprs.2009.07.001

Tiede, D., Hochleitner, G., Blaschke, T., 2005. A full GIS-based workflow for tree identification and tree crown delineation using laser scanning. Cmrt05, Iaprs 36, 9–14.

Vaccari, S., 2013. Virtual forests: terrestrial LiDAR as tool for improved tree modelling. Thesis Report GIRS-2013-03, Laboratory of Geo-Information Science and Remote Sensing 105.

Van der Werf, G.R., Morton, D.C., DeFries, R.S., Olivier, J.G.J., Kasibhatla, P.S., Jackson, R.B., Collatz, G.J., Randerson, J.T., 2009. CO2 emissions from forest loss. Nature Geoscience 2, 737–738. doi:10.1038/ngeo671

Wang, L., Gong, P., Biging, G.S., 2004. Individual Tree-Crown Delineation and Treetop Detection in High-Spatial-Resolution Aerial Imagery 3114, 351–358.

Wickham H.,2009. ggplot2: Elegant Graphics for Data Analysis. Springer-Verlag New York

Wulder, M. a., White, J.C., Niemann, K.O., Nelson, T., 2004. Comparison of airborne and satellite high spatial resolution data for the identification of individual trees with local maxima filtering. International Journal of Remote Sensing 25, 2225–2232. doi:10.1080/01431160310001659252

Xiao, W., 2012. Detecting changes in trees using multi-temporal airborne lidar point clouds 1.

Yao, W., Krzystek, P., Heurich, M., 2012. Tree species classification and estimation of stem volume and DBH based on single tree extraction by exploiting airborne full-waveform LiDAR data. Remote Sensing of Environment 123, 368–380. doi:10.1016/j.rse.2012.03.027

Yu, X., Hyyppä, J., Kukko, A., Maltamo, M., Kaartinen, H., 2006. Change detection techniques for canopy height growth measurements using airborne laser scanner data. Photogrammetric Engineering & Remote Sensing 72, 1339–1348. doi:10.14358/PERS.72.12.1339

Zawawi, A.A., Shiba, M., Janatun, N., Jemali, N., 2015. Accuracy of LiDAR-based tree height estimation and crown recognition in a subtropical evergreen broad-leaved forest in Okinawa , Japan 24, 1–11.

Zhang, C., Zhou, Y., Qiu, F., 2015. Individual Tree Segmentation from LiDAR Point Clouds for Urban Forest Inventory. Remote Sensing 7, 7892–7913. doi:10.3390/rs70607892

Appendices

Appendix 1- Field survey measurements of the study plot

Table 4. Tree species composition in plot Th01

Local Name	Botanical Name	Family Group	Number of trees	% in plot
Ubar	Syzygium	Non-Dipterocarpaceae	35	15.69507
Samak	Mezzettia parviflora Becc.	Non-Dipterocarpaceae	20	8.96861
Pelawan	Tristaniopsis whiteana (Griff.) Peter G. Wilson & J.T. Waterh.	Non-Dipterocarpaceae	16	7.174888
Jingjit	Calophyllum hosei Ridl.	Non-Dipterocarpaceae	14	6.278027
Meranti	Shorea parvifolia dyer	Dipterocarpaceae	13	5.829596
Perawas	Dehaasia caesia Bl.	Non-Dipterocarpaceae	10	4.484305
Terantang	Campnosperma coriaceum (Jack) Hall. f ex Steen.	Non-Dipterocarpaceae	10	4.484305
Asam asam putih	Tetractomia tetrandra (Roxb.) Merr.	Non-Dipterocarpaceae	9	4.035874
Medang	Rapanea borne+D50:H50ensis (Scheff.) Mez.	Non-Dipterocarpaceae	9	4.035874
Gelam tikus	Syzygium cf. cloranthum (Duthie) Merr. & L. M. Perry	Non-Dipterocarpaceae	7	3.139013
Jelutung	Alstonia pneumatophora Backer ex Den Berger	Non-Dipterocarpaceae	7	3.139013
Nyatok Babi	Palaquium cf. ridleyi King & Gamble	Non-Dipterocarpaceae	6	2.690583
Gandis	Garcinia rostrata Hassk ex. Hook. f.	Non-Dipterocarpaceae	5	2.242152
Gelam	Melaleuca leucadendra	Non-Dipterocarpaceae	5	2.242152
Kayu darah	Horsfieldia crassifolia (Hook. f & Thomson) Warb.	Non-Dipterocarpaceae	5	2.242152
Punak	Tetramerista glabra Miq.	Non-Dipterocarpaceae	5	2.242152
Bunyau	Aglaia rubiginosa (Hiern.) Pannell	Non-Dipterocarpaceae	4	1.793722
Darah darah	Horsfieldia crassifolia (Hook. f & Thomson) Warb.	Non-Dipterocarpaceae	4	1.793722
Jangkang	Xylopia fusca Maingayi ex Hook. f & Thomson	Non-Dipterocarpaceae	4	1.793722
Pampaning	Lithocarpus dasystacys (Miq.) Rehd.	Non-Dipterocarpaceae	4	1.793722
Geronggang	Cratoxylon glaucum Korth.	Non-Dipterocarpaceae	3	1.345291
Mahabai	Mezzettia umbellata Becc.	Non-Dipterocarpaceae	3	1.345291
Ramin	Gonystylus bancanus (Miq.) Kurz	Non-Dipterocarpaceae	3	1.345291
Kayu harang	Diospyros pilosanthera Blanco	Non-Dipterocarpaceae	2	0.896861
Kemantau	Species 1	Non-Dipterocarpaceae	2	0.896861
Nyatok rimbang	Palaquium cf. ridleyi King & Gamble	Non-Dipterocarpaceae	2	0.896861
Papung	Sandoricum beccarianum	Non-Dipterocarpaceae	2	0.896861
Wansira	Species 2	Non-Dipterocarpaceae	2	0.896861
Bansira	Ilex hypoglauca (Miq.) Loes	Non-Dipterocarpaceae	1	0.44843
Kapas kapas	Blumeodendron tokbrai (Blume) Kurz.	Non-Dipterocarpaceae	1	0.44843
Kempas	Kompassia malaccensis Maing ex Benth.	Non-Dipterocarpaceae	1	0.44843
Ketiaw	Madhuca mottleyana (de Vriesse) Macbr.	Non-Dipterocarpaceae	1	0.44843
Medang kuning	Rapanea sp	Non-Dipterocarpaceae	1	0.44843
Puri	Diospyros evena Bakh.	Non-Dipterocarpaceae	1	0.44843
Resak	Species 4	Non-Dipterocarpaceae	1	0.44843
Sabura	Ternstroemia magnifica Stapf ex Ridl.	Non-Dipterocarpaceae	1	0.44843
Tempurung	Syzygium syzygioides	Non-Dipterocarpaceae	1	0.44843
Tumih	Combretocarpus rotundotus	Non-Dipterocarpaceae	1	0.44843
Tunjang bakai	Blumeodendron tokbrai (Blume) Kurz.	Non-Dipterocarpaceae	1	0.44843
Ubah putih	Species 3	Non-Dipterocarpaceae	1	0.44843

Table 5. Attribute table of the field survey trees shapefile.

FID	Shape	Plot	Plot2	Subplot	Local_name	Botanical1	Family_Gro	Circumfere	DBH_	DBH	X__m_	Y_m_	xCrown__m_	yCrown_m_	Remarks	Meter	DBH_cm
20	Point	1	1	A	Ubar merah	Syzygium glaucum	Non-Dipterocarpaceae	44.2	14.07643	0	3.72	11.24	0	0	lean	0.14076	0.14076
21	Point	1	1	A	Gelam tikus	Syzygium cloranthum	Non-Dipterocarpaceae	36	11.46496	0	5.22	11.11	0	0		0.11465	0.11465
22	Point	1	1	A	Asam asam putih	Tetractomia tetrandra	Non-Dipterocarpaceae	33	10.50955	0	1.6	12	2.1	2.3		0.10509	0.10509
23	Point	1	1	A	Tempurung	Syzygium syzygioides	Non-Dipterocarpaceae	62	19.74522	0	0.1	12	4.2	5.2		0.19745	0.19745
24	Point	1	1	A	Pelawan	Tristaniopsis whiteana	Non-Dipterocarpaceae	46.1	14.68152	0	0.9	12.42	0	0	stem defect	0.14681	0.14681
25	Point	1	1	A	Gelam tikus	Syzygium cloranthum	Non-Dipterocarpaceae	49.9	15.89172	0	2.7	14.92	0	0		0.15891	0.15891
26	Point	1	1	A	Perawas	Dehaasia caesia	Non-Dipterocarpaceae	43.3	13.78980	0	4.4	18.2	0	0		0.13789	0.13789
27	Point	1	1	A	Samak	Mezzettia parviflora	Non-Dipterocarpaceae	48.7	15.50955	0	2	19.59	0	0		0.15509	0.15509
28	Point	1	1	A	Medang	Rapanea borneensis	Non-Dipterocarpaceae	59.8	19.04458	0	7.64	18.86	0	0		0.19044	0.19044
29	Point	1	1	A	Nyatok rimbang	Palaquium ridleyi	Non-Dipterocarpaceae	69.3	22.07006	0	8.88	18.84	7.1	7.3		0.22070	0.22070

Appendix 2 – Data co-registration

```
Final RMS: 1.43668 (computed on 50000 points)
----------------
Transformation matrix
0.972   -0.234  -0.000  4.051
0.233   0.970   0.070   -11.495
-0.016  -0.068  0.998   -7.060
0.000   0.000   0.000   1.000
----------------
Scale: fixed (1.0)
----------------
Theorical overlap: 100%
----------------
This report has been output to Console (F8)
```

Figure 41. Co-registration result after applying the ICP algorithm on PPC and TLS point cloud.

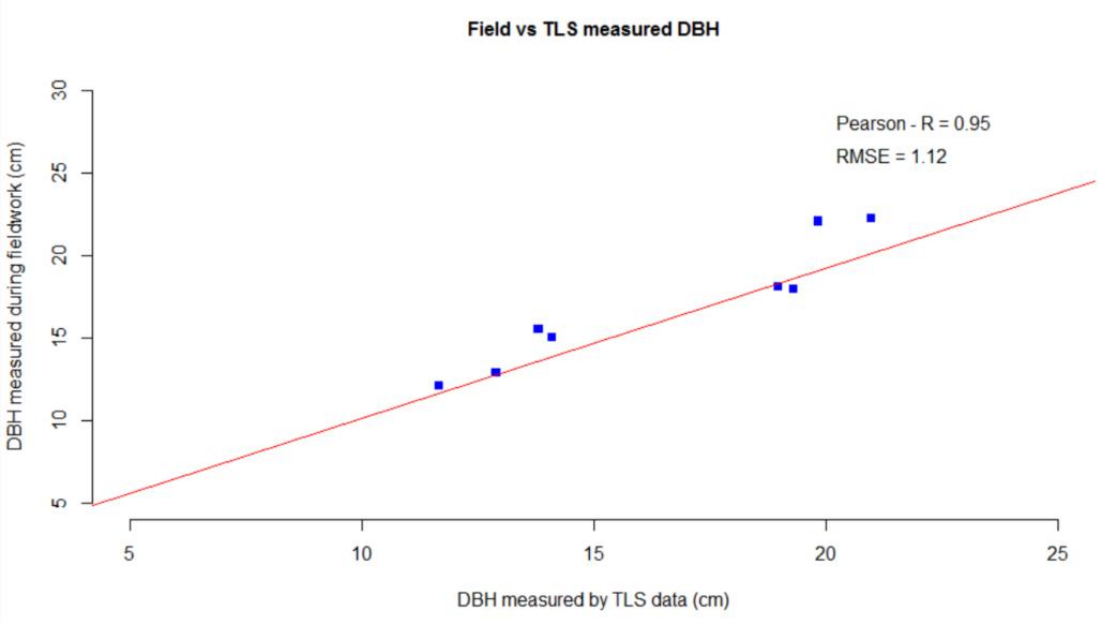

Figure 42.Correlation between field and TLS DBH for eight randomly selected trees, for assessing co-registration, RStudio.

Appendix 3. Polygon clean-up result in ArcMap

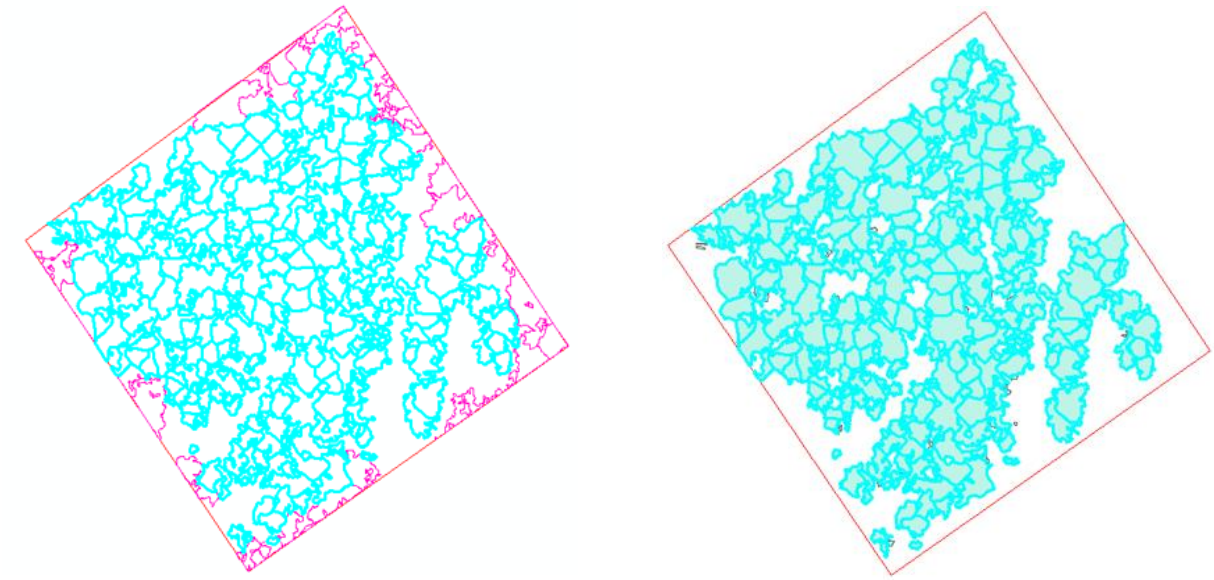

Figure 43. Left. Filtering out tree crowns intersecting with boundaries. Right. Calculating crown area (keep only > 0.45m^2)

Appendix 4. Point cloud segmentation based on PolyClipData – FUSION

(Runtime: 66 sec)

This algorithm can run either directly from command prompt or through software packages as R and Matlab (McGaughey, 2015). The following syntax is used to specify the function, the switch, the shapefile, the output folder and input file:

```
Cd C:
C:\FUSION\polyclipdata /multifile c:\shapefile\ITC.shp c:\las\clip_data.las
C:\las\UAVTh01Plot.las
```

The 'multifile' switch allows the creation of separate output data files for each polygon in the shapefile, so each tree in this phase can have its own RGB and TLS point cloud representation.

Appendix 5. Matlab code for hemi-ellipsoid fitting approach

1)

```
%% set directory and rename files 1 to 001 so to get correct file when asking
for it - This is only needed to run once in the beginning separately.

FileDetails = dir('*.las');
LasFileList = {FileDetails.name};
for i = 1:numel(LasFileList)  % Loop over the file names
  newName = sprintf('UAVTree%03d.las',i);  % Make the new name
  movefile(LasFileList{i},newName);        % Rename the file
end
```

2)

```
%% Clear the workspace and commands

clear all;
close all;

%% List all las files in folder

DataDir = 'D:\UAV';
OutputDir = 'D:\UAV\output_Sheng';
mkdir(OutputDir)
FileDetails = dir(fullfile(DataDir, '*.las'));

LasFileList = {};
for i=1:numel(FileDetails)
    LasFileList{i,1} = fullfile(DataDir, FileDetails(i).name);
end

% define file
OutputFile = fullfile(OutputDir, 'EllipsoidFitParameters.txt');
% init the output file
fid = fopen(OutputFile, 'w');
fprintf(fid, '%s\t%s\t%s\t%s\t%s\t%s\t%s\r\n', ...
    'file', 'ch', 'cr', 'cc', 'Xt', 'Yt', 'Zt');
fclose(fid);

%%
% Process each file
 for FileNum = 1:numel(LasFileList)
    % get filename as string
    LasFile =  LasFileList{FileNum};
    [~,filebasename] = fileparts(LasFile);
    disp(LasFile);

    % load here the data
    c = lasdata(LasFile);

    % Scale the data for visualization issues and create necessary input for
the ellipsoid
    MeanX = mean(c.x);
    MeanY = mean(c.y);
```

```
    x = c.x -MeanX;
    y = c.y -MeanY;
    z = c.z;

    % do the raster filtering
    FilterPixSize = 0.25;
    % build X and Y grid for the pixel grid of top of canopy
    [XX,YY] = meshgrid(min(x):FilterPixSize:max(x),
min(y):FilterPixSize:max(y));
    ZZ = nan(size(XX));
    % loop through each pixel
    for xi= 1:size(XX,2);
        for yi= 1:size(YY,1);
            % get pixel center coordinates
            x_pix = XX(yi,xi);
            y_pix = YY(yi,xi);
            % find the highest point cloud point within the pixel
            new_z = max(z((abs(x-x_pix)<=FilterPixSize/2) & (abs(y-
y_pix)<=FilterPixSize/2)));
            % if a point was inside the pixel...
            if ~isempty(new_z)
                % store it in output
                ZZ(yi,xi) = new_z;
            end
        end
    end

    % function to calculate Z value for the Sheng et al ellipsoid model.
    % The last part "0/..." is there to produce NaN values outside of the
    % ellipsoid
    % the crownheigh and cr are forced positive by abs
    Z_ShengFnc = @(x,y,ch,cr,cc,Xt,Yt,Zt) real(((1-((x-Xt).^2+(y-
Yt).^2).^(cc/2)/(abs(cr)^cc)).^(1/cc))*abs(ch) -abs(ch)+Zt) +
(0./(cr>sqrt((x-Xt).^2+(y-Yt).^2)));

    % Initial values for the [ch,cr,cc,Xt,Yt,Zt]-parameters
    p0 = [max(ZZ(:))-min(ZZ(:)), ... % crown height as difference between
highest and lowest Z value in data
        (max(XX(:))-min(XX(:)))/2, ... % crown radius from size of the area
        1, ... % curvature as constant
        mean(XX(:)), ... % center point as center of area
        mean(YY(:)), ... % center point as center of area
        max(ZZ(:))];    % tree height as the highest point in data
    % find the set of model parameters with minimum error in fit
    p = fminsearch(@(p)
CalculateFitQuality(ZZ,Z_ShengFnc(XX(:),YY(:),p(1),p(2),p(3),p(4),p(5),p(6)))
, p0);
    % Calculate fitted ZZ surface
    ZZZ = Z_ShengFnc(XX,YY,p(1),p(2),p(3),p(4),p(5),p(6));
    % visualize
    figure(196151289)
    clf

    subplot(2,2,1)
    plot(x, z, 'k.')
    hold on
```

```
    plot(XX,ZZ, 'mo')
    plot(XX,ZZZ, 'r*')
    title(['XZ ', filebasename], 'interpreter', 'none')
    axis equal
    xlabel('XYZ')

    subplot(2,2,2)
    plot(y, z, 'k.')
    hold on
    plot(YY,ZZ, 'mo')
    plot(YY,ZZZ, 'r*')
    title('YZ')
    axis equal

    subplot(2,2,3)
    plot(x, y, 'k.')
    hold on
    plot(XX,YY, 'mo')
    title('XY')
    axis equal

    subplot(2,2,4);
    hold on
    % draw point cloud
    plot3(x,y,z, 'k.')
    plot3(XX,YY,ZZ, 'mo')
    % draw ellipsoid center
    plot3(center(1),center(2),center(3), 'ro')
    mesh(XX,YY,ZZZ, 'FaceAlpha',0, 'LineWidth', 2)
    axis vis3d
    axis equal
    campos([min(xlim), min(ylim), max(zlim)])
    camlookat(gca)
    % write the picture
    print('-dpng', '-r300', fullfile(OutputDir,[filebasename, '_preview.png'
]));

    % write output
    fid = fopen(OutputFile, 'a');
    fprintf(fid, '%s\t%.3f\t%.3f\t%.3f\t%.3f\t%.3f\t%.3f\r\n', ...
        filebasename, p(1), p(2), p(3), p(4),p(5), p(6));
    fclose(fid);
end

%% visualiaze
    figure()
    clf
    hold on
    plot3(x_n,y_n,z_n, 'b.')
    plot3(center(1),center(2),center(3), 'ro')
     [ellX,ellY,ellZ] =
ellipsoid(center(1),center(2),center(3),radii(2),radii(3),radii(1),20);
    surf(ellX,ellY,ellZ)
    axis vis3d
    axis equal
```